

# Quark Number Fluctuations in a Chiral Model at Finite Baryon Chemical Potential

C. Sasaki,<sup>1</sup> B. Friman,<sup>1</sup> and K. Redlich<sup>2</sup>

<sup>1</sup>*Gesellschaft für Schwerionenforschung, GSI, D-64291 Darmstadt, Germany*

<sup>2</sup>*Institute of Theoretical Physics, University of Wrocław, PL-50204 Wrocław, Poland*

(Dated: May 18, 2018)

We discuss the net quark and isovector fluctuations as well as off-diagonal quark flavor susceptibilities along the chiral phase transition line in the Nambu–Jona-Lasinio (NJL) model. The model is formulated at non-zero quark and isospin chemical potentials with non-vanishing vector couplings in the iso-scalar and iso-vector channels. We study the influence of the quark chemical potential on the quark flavor susceptibilities in detail and the dependence of the results on model parameters as well as on the quark mass. The NJL model findings are compared with recent lattice results obtained in two-flavor QCD at finite chemical potential. On a qualitative level, the NJL model provides a consistent description of the dependence of quark number fluctuations on temperature and baryon chemical potential. The phase diagram and the position of the tricritical point in the NJL model are also discussed for different parameter sets.

PACS numbers: 24.60.Ky, 12.39.Fe, 12.38.Aw

## 1. INTRODUCTION

During recent years the phenomenological importance of fluctuations in finite temperature/finite density QCD has been widely recognized [1]. The analysis of fluctuations is a powerful method for characterizing the thermodynamic properties of a system. In particular, enhanced fluctuations are an essential characteristic of phase transitions [2, 3, 4, 5, 6, 7, 8]. Therefore, modifications in the magnitude of fluctuations have been suggested as a phenomenological probe of deconfinement and chiral symmetry restoration in heavy-ion collisions [1, 9]. In this context, fluctuations related to conserved charges, like baryon number, electric charge and isospin, are particularly relevant [1]. This is due mainly to the difference in mass gap of the effective degrees of freedom in the confined (hadronic) and deconfined (quark–gluon plasma) phases. Thus, a large change in charge fluctuations is to be expected when a system is passing from quark–gluon plasma to hadronic medium [1, 9]. In heavy ion collisions fluctuations may also reveal information on expansion dynamics of the medium created in the initial state and its electromagnetic emissivity as the fluctuations of isospin charge are connected with space-like screening limit of the retarded photon self-energy [10].

A measure of the intrinsic statistical fluctuations in a system close to thermal equilibrium is provided by the corresponding susceptibilities  $\chi$ . Hence, fluctuations in a thermodynamic system may be explored, at least in a limited scope, by finding the dependence of  $\chi$  on the thermal parameters. The properties of a strongly interacting statistical system are characterized by the temperature and a set of chemical potentials. The latter are related to the conservation laws, which follow from the global symmetries of QCD. For an isospin symmetric and electrically neutral system the thermodynamical ensemble depends only on two parameters, the temperature  $T$  and the quark chemical potential.

One of the consequences of QCD is the existence of a phase transition between the confined, chirally broken hadronic phase and the deconfined, chirally symmetric quark-gluon plasma phase. The two phases are separated by a phase boundary in the  $(T, \mu_q)$ -plane. The existence of the phase boundary for  $0 \leq \mu_q/T \leq 1$  has recently been established by first principle Lattice Gauge Theory (LGT) calculations at finite baryon chemical potential [11, 12, 13, 14].

Arguments based on effective models [15, 16, 17, 18, 19, 20, 21, 22] indicate that at large  $\mu_q$  the transition is first order. On the other hand, for small  $\mu_q$  and two massless quark flavors, the chiral transition is expected to be second order with the critical exponents of the O(4) spin model [23]. For finite quark masses, the second order transition is, due to explicit chiral symmetry breaking, most probably replaced by a rapid crossover. The different nature of the phase transition at low and high  $\mu_q$  suggests that the QCD phase diagram should exhibit a critical end point (CEP), where the line of first order phase transitions end. Beyond the critical end point the transition would then be continuous, i.e., second order or crossover. The critical properties of the second order critical end point are expected to be determined by the Ising model universality class [20, 24].

The existence of a critical end point in QCD has been recently studied in lattice calculations at non-vanishing chemical potential by either considering the location of Lee–Yang zeros in (2+1)-flavor QCD [11, 25] or by analyzing the convergence radius of the Taylor series for the free energy in 2-flavor QCD [12, 26]. Recent results [11] obtained within the first approach suggest that a critical endpoint indeed exists and that it is located at  $T \simeq 164$  and  $\mu_q \simeq 120$  MeV. On the other hand, in ref. [26] no direct evidence for the existence of a critical endpoint has been found in

2-flavor QCD with relatively large quark masses, in the range where the Taylor expansion is applicable, i.e., for  $\mu_q < T$ .

The critical behavior and the position of the critical end point can also be extracted from observables, that reflect the singular part of the free energy. Such an observable is the quark susceptibility  $\chi_{ij}$ , defined as the second derivative of the thermodynamical potential  $\Omega(T, \vec{\mu}, V)$  with respect to quark-flavor chemical potential  $\mu_f$ ,

$$\chi_{ff'} = -\frac{1}{V} \frac{\partial^2 \Omega}{\partial \mu_f \partial \mu_{f'}}, \quad (1.1)$$

where for two light (u,d)-quarks,  $\vec{\mu} = (\mu_u, \mu_d)$ . In particular, it was recently argued that the net quark number susceptibility  $\chi_q$  may be used to identify the chiral critical point in the QCD phase diagram [6, 7, 27]. The flavor off-diagonal susceptibility was also investigated at finite temperature in perturbative QCD [28]. In two-flavor QCD, for an isospin symmetric system,  $\chi_q$  is given by the sum of the  $uu$  and  $ud$  susceptibilities:  $\chi_q = 2(\chi_{uu} + \chi_{ud})$ . According to universality arguments,  $\chi_q$  diverges at the critical end point in the chiral limit as well as for finite quark masses, while away from the critical end point, the net quark number fluctuations are expected to be finite. Consequently, one expects a non-monotonic structure in  $\chi_q$  along the phase boundary if the QCD phase diagram features a critical end point.

The quark susceptibilities have been computed also in lattice QCD [13, 26, 29, 30]. Recently results for the quark number and isovector susceptibilities, or equivalently for the diagonal and off-diagonal quark flavor susceptibilities have been obtained on a lattice with two light quark flavors using a p4-improved staggered fermion action with a quark mass  $m_q/T = 0.4$  [12, 26]. Results for finite quark chemical potential were obtained by means of a Taylor series expansion. The susceptibilities were calculated up to fourth order in the quark chemical potential [26, 31, 32].

In general the net quark number susceptibility  $\chi_q$  shows a strong suppression of the corresponding fluctuations in the confined phase and a strong increase with temperature near the transition temperature  $T_0$ . Furthermore, the susceptibility near the transition temperature  $T_0$  shows a strong increase with increasing quark chemical potential, leading to cusp-like structure at  $\mu_q \simeq T$ . Besides, the lattice results confirm the expectation that the isovector quark susceptibility  $\chi_I$  does not exhibit a peaked structure near the transition temperature and shows rather weak dependence on  $\mu_q$ . This behavior of the susceptibilities is consistent with the existence of a singularity of the thermodynamic potential close to  $\mu_q = T = T_0$ , the chiral end point. However, the enhancement of  $\chi_q$  at finite  $\mu_q$  below the transition temperature can also be interpreted in terms of an enhanced contribution from baryon resonances; a very good description of the  $T$  and  $\mu_q$  dependences of the various quark susceptibilities in the confined phase is provided by the resonance gas partition function [26, 31, 32, 33].

Lattice calculations also show a strong correlation between fluctuations in different flavor components. This is particularly clear in the LGT results for the off-diagonal susceptibility  $\chi_{ud}$ , which shows a strong increase of  $u$ - $d$  correlations near the transition temperature  $T_0$  and an abrupt loss of correlations just above  $T_0$  [26, 31, 32].

In this paper we explore the properties of different quark susceptibilities in terms of an effective chiral model. Of particular interest is the characteristics of the quark number susceptibilities in different channels along the phase boundary and in the vicinity of the critical end point. The calculations will be done in the two-flavor Nambu-Jona-Lasinio (NJL) model [34] formulated at finite temperature and chemical potentials for the baryon number and isospin densities.

The NJL model has been used as a model for exploring qualitative features of the restoration of chiral symmetry in QCD [16, 35, 36, 37, 38]. In the particular case of  $SU_c(2)$  color symmetry this model has been recently argued to provide a realistic description of some of the lattice results [39]. However, in the  $SU_c(3)$  case it is rather unlikely that the NJL model can provide a quantitative understanding of LGT thermodynamics, since it does not exhibit confinement.<sup>#1</sup> Consequently, the hadronic degrees of freedom, in particular the baryonic resonances, which provide a quantitative interpretation of the LGT results in the confined phase [31, 32], are missing in the model. Furthermore, there are no gluon degrees of freedom in the NJL model. In QCD thermodynamics, in the chirally symmetric/deconfined phase, the gluons play an essential rôle. Finally, the model suffers from a strong dependence on the ultra-violet cut-off.

In the chiral limit, the phase diagram of the NJL model shows a phase separation line, where the spontaneously broken chiral symmetry is restored. At small densities the transition is second order, while for an appropriate choice of the coupling constants, the transition at large densities is first order. Thus, the model reproduces the gross structure of the phase diagram expected for QCD. Consequently, the NJL model, formulated at finite  $T$  and  $\vec{\mu}$ , can be used to explore the qualitative behavior of quark susceptibilities and, more generally, universal features of the chiral phase transition in the  $(T, \mu_q)$ -plane.

---

<sup>#1</sup> Recently an interesting extension of the NJL model was proposed that mimics confinement by including the Polyakov line as dynamical field which couples to constituent quarks [40].

The net quark number susceptibility has been computed in the NJL model at finite  $T$  some time ago [2] and recently also at finite quark chemical potential  $\mu_q$  [7]. Our analysis is going beyond previous studies by extending the NJL Lagrangian to finite quark and isospin chemical potential as well as to non-vanishing vector coupling among the constituent quarks. This allows us to model the net quark number susceptibility  $\chi_q$ , the isovector one  $\chi_I$  or equivalently the diagonal and off-diagonal quark flavor susceptibilities  $\chi_{ff'}$  and to study their dependence on temperature and chemical potential as well as on model parameters. On a qualitative level the results can then be confronted with recent lattice results.

The paper is organized as follows: In section 2, we introduce the NJL model Lagrangian and its thermodynamics. In section 3, we introduce the flavor diagonal and off-diagonal susceptibilities and calculate their  $T$  and  $\mu_q$  as well as model parameters dependences. We discuss the qualitative comparison of the model results with the recent lattice findings. Finally in section 4, we give a brief summary and discussion of our results.

## 2. THE TWO-FLAVOR NJL MODEL

For two quark flavors and three colors the Lagrangian of the Nambu–Jona-Lasinio (NJL) model reads [16, 35, 37, 38]:

$$\begin{aligned} \mathcal{L} = & \bar{\psi}(i\cancel{\partial} - m)\psi + G_S \left[ (\bar{\psi}\psi)^2 + (\bar{\psi}i\vec{\tau}\gamma_5\psi)^2 \right] \\ & - G_V^{(S)} (\bar{\psi}\gamma_\mu\psi)^2 - G_V^{(V)} \left[ (\bar{\psi}\vec{\tau}\gamma_\mu\psi)^2 + (\bar{\psi}\vec{\tau}\gamma_\mu\gamma_5\psi)^2 \right] + \bar{\psi}\mu\gamma_0\psi, \end{aligned} \quad (2.1)$$

where  $m = \text{diag}(m_u, m_d)$  is the current quark mass matrix,  $\mu = \text{diag}(\mu_u, \mu_d)$  the chemical potential matrix and  $\vec{\tau}$  denotes Pauli matrices. The strength of the interaction between the constituent quarks in the scalar and vector channels is parameterized by the dimensionful coupling constants  $G_S$ ,  $G_V^{(S)}$  and  $G_V^{(V)}$ . We note that while the strength of the scalar-isoscalar and pseudoscalar-isovector interactions are equal, due to constraints from chiral symmetry, the vector-isoscalar and vector-isovector interaction terms are separately invariant, and hence the corresponding interaction strengths can be chosen independently. In the following calculations focused on the quark number susceptibility, we choose the axial-vector condensate to be zero since it does not couple to the vector current.

The constraints imposed by the conservation of the net quark number of different flavors are controlled by the chemical potential  $\mu = \text{diag}(\mu_u, \mu_d)$ . The chemical potentials for the total net quark density  $n_q$  and the iso-vector quark density  $n_I$  are obtained as linear combinations of  $\mu_u$  and  $\mu_d$

$$\mu_q = \frac{1}{2}(\mu_u + \mu_d), \quad \mu_I = \frac{1}{2}(\mu_u - \mu_d). \quad (2.2)$$

In terms of  $\mu_q$  and  $\mu_I$ , the last term of the Lagrangian can be expressed as

$$\mathcal{L}_\mu = \bar{\psi}\mu\gamma_0\psi = \mu_q\psi^\dagger\psi + \mu_I\psi^\dagger\tau_3\psi. \quad (2.3)$$

In addition to the current quark masses and the three coupling constants introduced above, one additional parameter is required to complete the model. This is the momentum cut-off ( $\Lambda$ ), which regulates the ultraviolet divergencies. In vacuum the values of  $\Lambda$  and  $G_S$  are fixed by requiring that the pion decay constant  $f_\pi = 92.4$  MeV and the pion mass  $m_\pi = 135$  MeV are reproduced. Choosing the current quark masses  $m_u \simeq m_d = 5$  MeV one finds for a three-momentum cutoff  $\Lambda = 664.3$  MeV and  $G_S\Lambda^2 = 2.06$  [38].

In the chirally broken phase, the ratio of the coupling constants of  $\omega$  and  $\rho$  mesons to nucleons is empirically given by  $g_{\omega NN}/g_{\rho NN} \simeq 3$ . This value is also consistent with the naive quark model for the nucleon, where the corresponding couplings to quarks are identical, i.e.,  $g_{\omega QQ}/g_{\rho QQ} = 1$ . We account for this on a qualitative level by setting  $G_V^{(S)} \simeq 3G_V^{(V)}$  in the broken phase and  $G_V^{(S)} = G_V^{(V)}$  in the symmetric phase. Thus, we consider  $G_V^{(V)}/G_V^{(S)}$  in the range from  $\frac{1}{3}$  to 1, keeping the vector-isoscalar coupling fixed  $G_V^{(S)} = 0.3G_S$ .

The thermodynamics of the NJL model (2.1) at finite temperature and non vanishing net quark and isospin chemical potentials is obtained from the partition function  $Z(T, \mu_q, \mu_I, V)$ . In the mean field approximation [16] the partition function is obtained from the effective Lagrangian

$$\begin{aligned} \mathcal{L} = & \bar{\psi}(i\cancel{\partial} - M + \tilde{\mu}\gamma_0)\psi - \frac{1}{4G_S}\text{tr}((M - m)^2) \\ & + \frac{1}{4G_V^{(S)}}(\tilde{\mu}_q - \mu_q)^2 + \frac{1}{4G_V^{(V)}}(\tilde{\mu}_I - \mu_I)^2, \end{aligned} \quad (2.4)$$

where  $M = \text{diag}(M_u, M_d)$  and the trace  $\text{tr}$  is in flavor space.

In Eq. (2.4) we have introduced a dynamical mass  $M$  and a shifted chemical potential  $\tilde{\mu}$  given by

$$M = m - 2G_S \langle \bar{\psi} \psi \rangle, \quad (2.5)$$

$$\tilde{\mu} = \tilde{\mu}_q + \tilde{\mu}_I \tau_3, \quad (2.6)$$

where

$$\begin{aligned} \tilde{\mu}_q &= \mu_q - 2G_V^{(S)} \langle \bar{\psi} \gamma_0 \psi \rangle, \\ \tilde{\mu}_I &= \mu_I - 2G_V^{(V)} \langle \bar{\psi} \tau_3 \gamma_0 \psi \rangle. \end{aligned} \quad (2.7)$$

The resulting thermodynamic potential density<sup>#2</sup> is of the following form

$$\begin{aligned} \omega(T, \mu; M, \tilde{\mu}) &= \sum_{f=u,d} \omega_f(T, \mu; M_f, \tilde{\mu}_f) + \frac{1}{4G_S} \text{tr}((M - m)^2) \\ &\quad - \frac{1}{4G_V^{(S)}} (\tilde{\mu}_q - \mu_q)^2 - \frac{1}{4G_V^{(V)}} (\tilde{\mu}_I - \mu_I)^2, \end{aligned} \quad (2.8)$$

where

$$\begin{aligned} \omega_f(T, \mu; M_f, \tilde{\mu}_f) &= -2N_c \int \frac{d^3p}{(2\pi)^3} \left[ E_f(\vec{p}) - T \ln(1 - n_f^{(+)}(\vec{p}, T, \tilde{\mu}_f)) \right. \\ &\quad \left. - T \ln(1 - n_f^{(-)}(\vec{p}, T, \tilde{\mu}_f)) \right]. \end{aligned} \quad (2.9)$$

In Eq. (2.9),  $E_f(\vec{p}) = \sqrt{\vec{p}^2 + M_f^2}$  is the scalar part of the quasiparticle energy. The contributions of the vector potentials are absorbed in the shifted chemical potential  $\tilde{\mu}_f$ . Furthermore,  $n_f^{(\pm)}$  is the distribution function for particle (+) and anti-particle (-) states

$$n_f^{(\pm)}(\vec{p}, T, \tilde{\mu}_f) = \left( 1 + \exp[(E_f(\vec{p}) \mp \tilde{\mu}_f)/T] \right)^{-1}. \quad (2.10)$$

The condensates appearing in Eqs. (2.6)-(2.8) are determined by extremizing the thermodynamic potential<sup>#3</sup> with respect to the dynamical mass and the shifted chemical potentials at a given temperature  $T$  and chemical potential  $\mu$

$$\frac{\partial \omega}{\partial M} = \frac{\partial \omega}{\partial \tilde{\mu}_q} = \frac{\partial \omega}{\partial \tilde{\mu}_I} = 0. \quad (2.11)$$

These conditions yield the scalar condensate and the quark densities as functions of temperature and chemical potential. Furthermore, they imply that the scalar and vector fields can be fixed when computing thermodynamic derivatives. Thus, one obtains the standard thermodynamic relations for instance for the quark density

$$n_q = - \left. \frac{\partial \omega(T, \mu)}{\partial \mu} \right|_T = - \left. \frac{\partial \omega(T, \mu; M_f, \tilde{\mu}_f)}{\partial \mu} \right|_{T; M, \tilde{\mu}}. \quad (2.12)$$

However, as discussed below, the dependence of  $M$  and  $\tilde{\mu}$  on temperature and chemical potential yields non-trivial contributions to second derivatives of the thermodynamic potential, e.g., susceptibilities.

The stationarity conditions (2.11), together with Eqs. (2.6)-(2.8), imply

$$M_f = m_f + 4G_S N_c \sum_{f=u,d} \int \frac{d^3p}{(2\pi)^3} \frac{M_f}{E_f} \left[ 1 - n_f^{(+)}(\vec{p}, T, \tilde{\mu}_f) - n_f^{(-)}(\vec{p}, T, \tilde{\mu}_f) \right], \quad (2.13)$$

$$\mu_q = \tilde{\mu}_q + 4G_V^{(S)} N_c \sum_{f=u,d} \int \frac{d^3p}{(2\pi)^3} \left[ n_f^{(+)}(\vec{p}, T, \tilde{\mu}_f) - n_f^{(-)}(\vec{p}, T, \tilde{\mu}_f) \right], \quad (2.14)$$

$$\mu_I = \tilde{\mu}_I + 4G_V^{(V)} N_c \int \frac{d^3p}{(2\pi)^3} \left[ \left( n_u^{(+)}(\vec{p}, T, \tilde{\mu}_u) - n_u^{(-)}(\vec{p}, T, \tilde{\mu}_u) \right) - (u \rightarrow d) \right]. \quad (2.15)$$

<sup>#2</sup> The thermodynamic potential is given by  $\Omega = \omega V$ , where  $V$  is the volume of the system.

<sup>#3</sup> The thermodynamic potential is minimized with respect to variations of the scalar field and maximized with respect to variations of the (zeroth component) of the vector fields.

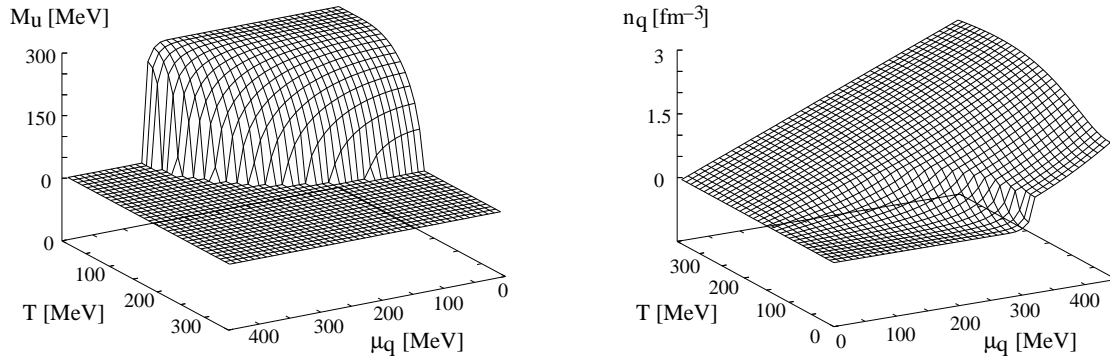


FIG. 1: The left-hand figure shows the dynamical u-quark mass  $M_u$  in the chiral limit as a function of temperature  $T$  and the quark chemical potential  $\mu_q$ . The right-hand figure represents the quark number density  $n_q$  in the chiral limit in the  $(T, \mu_q)$ -parameter space. The calculations were done for isospin symmetric matter, i.e.  $\mu_I = 0$ , with  $G_V^{(S)} = 0.3 G_S$ .

By comparing Eqs. (2.7), (2.14) and (2.15), we find explicit expressions for the quark number density  $n_q = \langle \bar{\psi} \gamma_0 \psi \rangle$  and the iso-vector density  $n_I = \langle \bar{\psi} \tau_3 \gamma_0 \psi \rangle$

$$n_q = 2N_c \sum_{f=u,d} \int \frac{d^3p}{(2\pi)^3} \left[ n_f^{(+)}(\vec{p}, T, \tilde{\mu}_f) - n_f^{(-)}(\vec{p}, T, \tilde{\mu}_f) \right], \quad (2.16)$$

$$n_I = 2N_c \int \frac{d^3p}{(2\pi)^3} \left[ \left( n_u^{(+)}(\vec{p}, T, \tilde{\mu}_u) - n_u^{(-)}(\vec{p}, T, \tilde{\mu}_u) \right) - (u \rightarrow d) \right]. \quad (2.17)$$

In practice, one first solves the gap equation (2.13) for fixed  $T$ ,  $\tilde{\mu}_q$  and  $\tilde{\mu}_I$  and then computes  $\mu_q$  and  $\mu_I$  as well as  $n_q$  and  $n_I$  using (2.14)-(2.17).

In Fig. 1 we show the dynamical quark mass  $M_f$  and the net quark number density  $n_q$  in the  $(T, \mu_q)$ -plane for vanishing iso-vector chemical potential  $\mu_I = 0$  in the chiral limit. For  $\mu_I = 0$  the isovector density  $n_I$  vanishes for all values of  $T$  and  $\mu_q$ . In Fig. 2 the phase diagram of the NJL model in the  $(T, \mu_q)$ -plane is shown for an isospin symmetric system in the limit of vanishing current quark masses. The boundary between the chirally broken and symmetric phases was located by finding the onset of chiral symmetry restoration,  $M(T, \mu_q) = 0$ , when approaching from the broken phase. As discussed in the introduction, the order of chiral phase transition is, in the chiral limit, expected to change from second order at low to first order at high net baryon densities. Thus, somewhere along the phase boundary one expects a tricritical point (TCP), where the order of the chiral transition changes. Close to the phase boundary, the thermodynamic potential, may be expanded in a power series in the order parameter  $M$  as in Landau theory [41]:  $\omega(T, \mu_q; M) = \omega_0 + \frac{1}{2}aM^2 + \frac{1}{4}bM^4 + O(M^6)$ . At a second-order transition  $a = 0$  and  $b > 0$ , while at a first order one  $a > 0$  and  $b < 0$ . (In the latter case, the coefficient of  $M^6$  should be positive for stability.) Thus, the tricritical point can be identified by  $a = b = 0$ .

In the NJL model the position of the phase boundary and the TCP depends on the model parameters [38, 42, 43, 44]. In Fig. 2 we illustrate the dependence on the vector and scalar couplings  $G_V^{(S)}$  and  $G_S$  as well as on the momentum cut-off  $\Lambda$ . In the left panel the critical line is shown for different strengths of the vector coupling  $G_V^{(S)}$ , keeping  $G_S$  and  $\Lambda$  fixed. With increasing  $G_V^{(S)}$ , the phase boundary at fixed  $T$  is shifted to larger  $\mu_q$ . This is expected, since at non-zero net baryon density, the vector coupling  $G_V^{(S)}$  provides a repulsive contribution to the energy of a quark and thus to the chemical potential (see Eqs. (2.7),(2.14)). In fact, in the  $T - \tilde{\mu}_q$  plane the position of the line of second order phase transitions is independent of  $G_V^{(S)}$ . This is clear from the fact that the gap equation Eq. (2.13) depends on  $G_V^{(S)}$  only through  $\tilde{\mu}_q$ . On the other hand, the location of the first order transition and the position of the TCP do depend on the vector coupling  $G_V^{(S)}$ . This dependence is reflected in the shift of the TCP to smaller temperatures with increasing strength of the vector coupling. We note that for  $G_V^{(S)} > 0.6 G_S$ , the transition is everywhere second order and there is no TCP. In the right panel of Fig. 2 we show the dependence of the phase boundary on the cut off  $\Lambda$ . We have chosen three parameter sets, summarized in Table I, where the cut off is varied from our standard value,  $\Lambda = 664.3$  MeV, up to almost 1 GeV, keeping  $G_V^{(S)} = 0$ . The corresponding values of  $G_S$  are chosen such that all

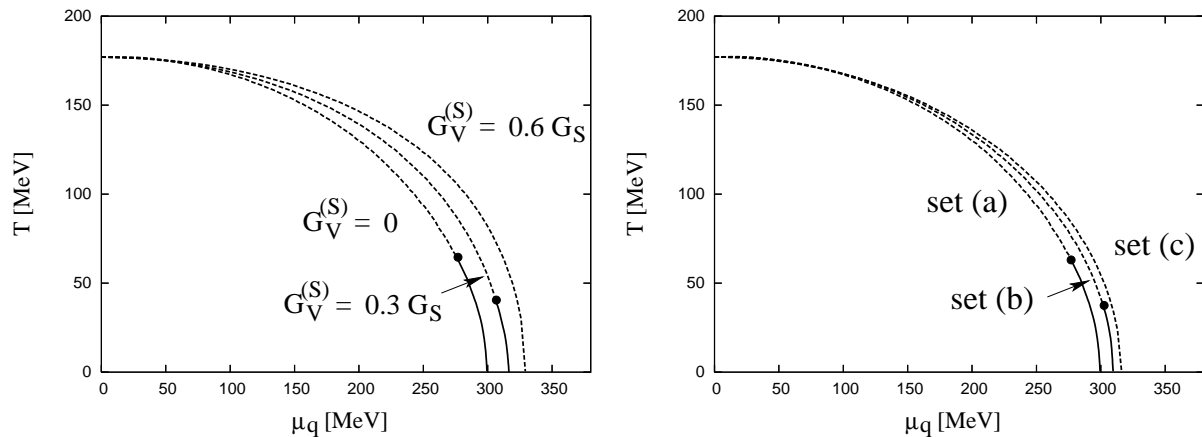


FIG. 2: The NJL model phase diagram in the chiral limit for  $G_V^{(S)} = 0, 0.3$  and  $0.6 G_S$  (left panel) and for the set of parameters (a)-(c) of Table. 1 (right panel). The dashed (solid) line shows the location of the second-order (first-order) transition. The tricritical point, indicated by a dot ( $\bullet$ ), is located at  $(T, \mu_q) = (65, 275)$  MeV for  $G_V^{(S)} = 0$  and at  $(T, \mu_q) = (42, 305)$  MeV for  $G_V^{(S)} = 0.3 G_S$ . Both phase diagrams correspond to a vanishing isovector chemical potential,  $\mu_I = 0$ .

	$\Lambda$ (MeV)	$G_S \Lambda^2$
set (a)	664.3	2.060
set (b)	797.2	1.935
set (c)	995.5	1.829

TABLE I: Set of cutoff  $\Lambda$  and scalar coupling constant  $G_S$  used in the model calculations.

parameter sets yield the same critical temperature at  $\mu_q = 0$ , i.e.  $T_c = 177$  MeV, in agreement with lattice results for two-flavor QCD [45]. With increasing  $\Lambda$ , the phase boundary is again shifted to slightly larger values of the chemical potential and the TCP to smaller temperatures.

In appendix A we give a closed expression for the integrals appearing in the gap equation (2.13) at the phase boundary. Furthermore, by requiring that the critical temperature at  $\mu = 0$  remains fixed, as in the right panel of Fig. 2, we obtain a relation between the chemical potential at the  $T = 0$  transition and the cut off  $\Lambda$

$$\delta\mu = \frac{2}{e^{\Lambda/T} + 1} \frac{\Lambda}{\mu} \delta\Lambda. \quad (2.18)$$

This relation is derived under the assumption that the transition is second order everywhere. Nevertheless, it is well satisfied also when the transition is weakly first order at high quark densities. Thus, (2.18) provides a quantitative interpretation of the shift of the phase boundary found in Fig. 2.

We conclude that in the limit of vanishing vector coupling, ( $G_V \rightarrow 0$ ), the TCP in the NJL model is located at  $T \simeq 65$  and  $\mu_q \simeq 275$  MeV. For non-zero  $G_V^{(S)}$  the position of the TCP moves towards lower temperature and higher chemical potential, and for sufficiently large vector coupling, the chiral transition is second-order everywhere.

The phase diagram in the  $(T, \mu_q)$ -plane shown in Fig. 2 applies to the chiral limit. A non-zero quark mass in the Lagrangian (2.4) will modify the position of the phase boundary. Furthermore, a finite quark mass breaks the chiral symmetry of the Lagrangian explicitly. Consequently, the second order transition at high  $T$  and small  $\mu$  is replaced by a cross-over transition and the TCP by a critical end point. The critical behavior of the NJL model for finite quark masses is consistent with the results obtained in other effective models [6, 17, 38, 42, 44].

The position of the phase boundary and the order of the chiral phase transition can be also identified through thermodynamic observables. In the Introduction we argued that quark number fluctuations are sensitive probes of the phase transition. Furthermore, fluctuations of conserved charges are directly accessible in experiments. Thus, it is of interest to explore the behavior of the quark number fluctuations in the vicinity of the phase boundary in effective models, like the NJL model.

In the next sections we formulate quark susceptibilities in the NJL model and explore their dependence on thermal



and model parameters. We also consider the influence of finite quark masses on the quark fluctuations and discuss the NJL model results in the context of the recent lattice findings.

### 3. QUARK NUMBER SUSCEPTIBILITIES

The net quark number and iso-vector susceptibilities  $\chi_q$  and  $\chi_I$  describe the response of the quark density  $n_q$  and the isovector density  $n_I$  to the change of the corresponding chemical potentials. Thus,  $\chi_q$  and  $\chi_I$  are defined as derivatives of  $n_q$  and  $n_I$  with respect to  $\mu_q$  and  $\mu_I$

$$\chi_q = \frac{\partial n_q}{\partial \mu_q}, \quad \chi_I = \frac{\partial n_I}{\partial \mu_I}. \quad (3.1)$$

The net quark and the isovector densities are in the NJL model given by Eqs. (2.16) and (2.17). The evaluation of the derivatives in (3.1), taking the implicit dependence of the dynamical masses  $M_f$  and the shifted chemical potentials  $\tilde{\mu}_f$  on  $\mu_q$  and  $\mu_I$  into account, yields

$$\begin{aligned} \chi_q = & \frac{2N_c}{T} \sum_{f=u,d} \int \frac{d^3p}{(2\pi)^3} \left[ -\frac{M_f}{E_f} \frac{\partial M_f}{\partial \mu_q} \left( n_f^{(+)}(1 - n_f^{(+)}) - n_f^{(-)}(1 - n_f^{(-)}) \right) \right. \\ & \left. + \frac{\partial \tilde{\mu}_f}{\partial \mu_q} \left( n_f^{(+)}(1 - n_f^{(+)}) + n_f^{(-)}(1 - n_f^{(-)}) \right) \right], \end{aligned} \quad (3.2)$$

$$\begin{aligned} \chi_I = & \frac{2N_c}{T} \int \frac{d^3p}{(2\pi)^3} \left[ -\frac{M_u}{E_u} \frac{\partial M_u}{\partial \mu_I} \left( n_u^{(+)}(1 - n_u^{(+)}) - n_u^{(-)}(1 - n_u^{(-)}) \right) \right. \\ & \left. + \frac{\partial \tilde{\mu}_u}{\partial \mu_I} \left( n_u^{(+)}(1 - n_u^{(+)}) + n_u^{(-)}(1 - n_u^{(-)}) \right) - (u \rightarrow d) \right]. \end{aligned} \quad (3.3)$$

In Eqs. (3.2) and (3.3) we have suppressed the  $T$  and  $\tilde{\mu}_f$  dependence of the distribution functions  $n_f^{(\pm)}$ . The derivatives of the dynamical masses  $M_f$  and the reduced chemical potentials  $\mu_f$  entering in Eqs. (3.2) and (3.3) are given in Appendix B.

In addition to the fluctuations of the net quark and isovector densities we also introduce the flavor diagonal and off-diagonal susceptibilities defined by

$$\chi_{ff} = -\frac{\partial^2 \omega}{(\partial \mu_f)^2}, \quad \chi_{ff'} = -\frac{\partial^2 \omega}{\partial \mu_f \partial \mu_{f'}}, \quad (3.4)$$

with  $f \neq f' \in \{u, d\}$ .

In isospin symmetric matter the susceptibilities  $\chi_{uu}(= \chi_{dd})$  and  $\chi_{ud}$  are related to  $\chi_q$  and  $\chi_I$  by

$$\chi_{uu} = \frac{1}{4}(\chi_q + \chi_I), \quad \chi_{ud} = \frac{1}{4}(\chi_q - \chi_I). \quad (3.5)$$

In the following section we compute the susceptibilities introduced in Eqs. (3.2)-(3.5) in the NJL model and discuss the dependence of the quark number fluctuations on temperature and chemical potentials in the vicinity of the phase boundary.

#### 3.1. Quark susceptibilities in the NJL model

As discussed above, the NJL model does not exhibit the confinement property of QCD. Thus, there are no hadronic bound states and resonances in the chirally broken phase. Instead we are dealing with constituent quarks which can be viewed as quasi-particles, with a temperature and density dependent mass. At the chiral transition the composition of the medium is not changed in the NJL model; the dynamical quark masses  $M_f$  vanish and above  $T_c$  the medium is populated by interacting massless quarks. Furthermore, high momentum quark modes are suppressed due to the ultra-violet cut-off. This suppression is particularly relevant at high temperatures. The differences in the mass spectrum between the NJL model and QCD, as well as the suppression of high-momentum states, results in different

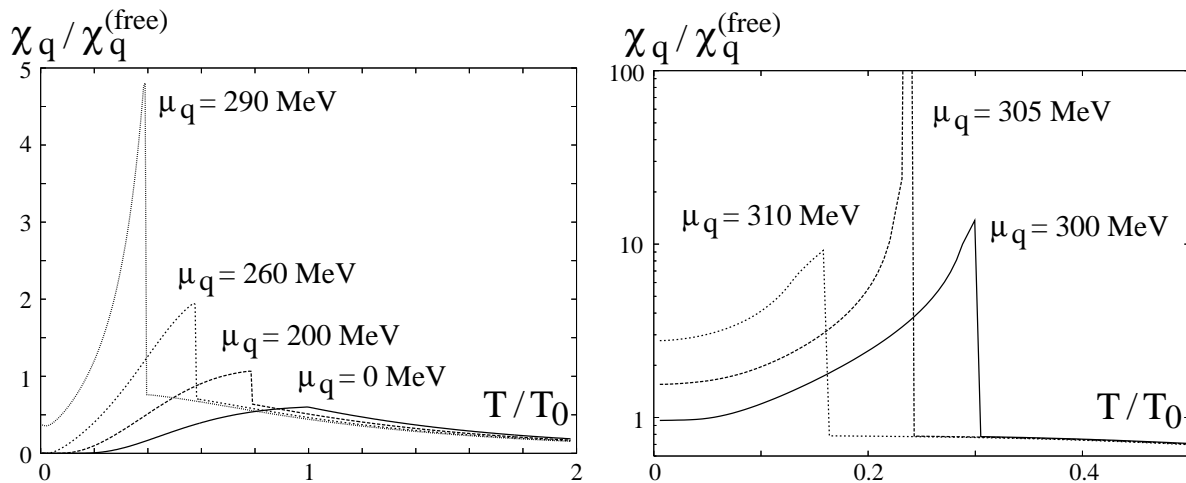


FIG. 3: The quark number susceptibility  $\chi_q$  as a function of  $T/T_0$  in the chiral limit, for different values of the quark chemical potential  $\mu_q$ . Here  $\chi_q^{(\text{free})}$  is the quark number susceptibility for an ideal quark gas and  $T_0 = 177$  MeV is the transition temperature at  $\mu_q = \mu_I = 0$ . The calculations correspond to an isospin symmetric system with  $G_V^{(S)} = 0.3 G_S$ .

quantitative properties of the quark number fluctuations. In spite of these differences, the NJL model is useful for exploring general features of the susceptibilities close to the phase boundary and, in particular, near the TCP.

In Fig. 3 we show the quark number susceptibility  $\chi_q$  as a function of  $T$  for different values of  $\mu_q$ , normalized to that of an ideal quark gas  $\chi_q^{(\text{free})} = N_c N_f (T^2/3 + \mu_q^2/\pi^2)$ .

The temperature dependence of  $\chi_q$  shows characteristic features, which vary rapidly with  $\mu_q$ . The phase boundary is signaled by a discontinuity in the susceptibility. The size of the discontinuity grows with increasing  $\mu_q$  up to the TCP, where the susceptibility diverges. Beyond the TCP the discontinuity is again finite. On the other hand, at  $\mu_q = 0$  the discontinuity vanishes and the susceptibility shows a weaker non-analytic structure at the transition temperature, corresponding to a discontinuity in  $\partial\chi_q/\partial T$ . The critical properties of  $\chi_q$  are consistent with a second order phase transition belonging to the universality class of  $O(4)$  spin model in three dimensions [6, 31]. Due to the lack of confinement in the NJL model, the leading contribution to the thermodynamic potential and to fluctuations of conserved charges is due to single-quark loops. The model can be improved by including the interaction of quarks with the Polyakov loops. In the resulting PNJL model [40, 46], confinement is mimicked in the sense that three-quark states are the leading thermodynamic modes below the phase boundary, in the “confined” phase. In this model the fluctuations of the net quark number in the chirally broken phase are suppressed [46] compared to the results of the NJL model shown in Fig. 3. Furthermore, in the PNJL model the dependence of the fluctuations on the value of the quark chemical potential is also stronger. Recently, it was shown [47] that by an appropriate choice of the parameterization of the effective Polyakov loop potential, it is possible to quantitatively reproduce some LGT results on fluctuations of conserved charges. Nevertheless, the critical properties of the net quark number fluctuations near the phase transition in the NJL and in PNJL models are similar, since both models belong to the same universality class.

We now explore the qualitative features of the critical region within Landau theory [41]. As already indicated in section 2, we construct an effective thermodynamic potential, valid in the vicinity of the chiral transition. The thermodynamical potential  $\omega(M, T, \mu_q)$  is expanded in a power series in the order parameter  $M$ , the dynamical quark mass, around  $M = 0$ :

$$\omega(T, \mu_q, M) \simeq \omega_0(T, \mu_q) + \frac{1}{2}a(T, \mu_q)M^2 + \frac{1}{4}b(T, \mu_q)M^4 + O(M^6). \quad (3.6)$$

Here we neglect the  $M^6$  term for simplicity. Although it is crucial for the calculation of critical exponents (see Appendix C), it does not affect the present argument. We assume that  $b \geq 0$ , i.e., that we are above or at the TCP, where the transition is second order. For  $a > 0$ , the effective potential (3.6) has a minimum at  $M = 0$ , which corresponds to the symmetric phase, where  $\omega(T, \mu; 0) = \omega_0(T, \mu)$ . On the other hand, for  $a < 0$  the minimum is located at  $M_0 = \sqrt{-a/b}$  and the system is in the broken symmetry phase, where

$$\omega(T, \mu_q; M_0) = \omega_0(T, \mu_q) - \frac{1}{4} \frac{a^2(T, \mu_q)}{b(T, \mu_q)}. \quad (3.7)$$



The second-order phase boundary (the  $O(4)$  critical line) is determined by the requirement  $a = 0$  and  $b \geq 0$ . Above the critical line, in the symmetric phase,  $M = 0$  and the quark number susceptibility  $\chi_q$  is given by

$$\chi_q^{(\text{sym})} = -\frac{\partial^2 \omega_0}{\partial \mu_q^2}. \quad (3.8)$$

The coefficient  $a(T, \mu_q)$  may be expanded around any point  $(T_c, \mu_c)$  on the  $O(4)$  critical line. Close to the critical line, it is sufficient to keep only the leading terms

$$a(T, \mu_q) \simeq A(T - T_c) + B(\mu_q - \mu_c), \quad (3.9)$$

where the expansion coefficients  $A$  and  $B$  depend on  $T_c$  and  $\mu_c$ .

Using Eqs. (3.7) and (3.9) obtains the quark susceptibility in the broken phase

$$\chi_q^{(\text{broken})} = \chi_q^{(\text{sym})} + \frac{B^2}{2b(T, \mu_q)}, \quad (3.10)$$

where we have dropped terms that vanish on the critical line. The discontinuity of  $\chi_q$  across the  $O(4)$  critical line at finite  $\mu_q$  is given by the second term in (3.10). At  $\mu_q = 0$  the coefficient  $B$ , and thus the discontinuity of  $\chi_q$ , vanishes by symmetry. Keeping the next term in the expansion of  $a(T, \mu_q) \simeq A(T - T_c) + B_2 \mu_q^2$ , one finds  $\chi_q^{(\text{broken})}(\mu_q = 0) = \chi_q^{(\text{sym})}(\mu_q = 0) + (T - T_c)AB_2/b$ . Thus, at  $\mu_q = 0$  the susceptibility at  $T = T_c$  is continuous, while its temperature derivative is discontinuous, as seen in Fig. 3.

Finally at the TCP both  $a(T, \mu_q)$  and  $b(T, \mu_q)$  vanish. Consequently, the susceptibility in the broken phase (3.10) diverges at the TCP, in agreement with the results shown in the right panel of Fig. 3. With the present choice of parameters, the TCP is located at  $(T_{\text{TCP}}, \mu_{\text{TCP}}) = (42, 305)$  MeV. Beyond the TCP, the phase transition is first order. There the susceptibility again exhibits a finite discontinuity at the phase boundary. The susceptibility in the symmetric phase,  $\chi_q^{(\text{sym})}$ , is expected to vary smoothly along the phase boundary.

From the perspective of heavy ion experiments, several susceptibilities are of interest. In particular, this applies to fluctuations of conserved charges, which may be directly accessible in experiment. Furthermore, those susceptibilities that reflect the critical behavior, may possibly be used to explore the QCD phase transition experimentally. As we have stressed repeatedly, the quantitative structure of the phase diagram and the position of the critical end point are model dependent. Consequently, in detail the QCD phase diagram most likely differs from that found in the NJL model. Nevertheless, such a model study can still answer phenomenologically relevant questions concerning e.g. the size of the critical region, where the fluctuations are dominated by the singularity at the conjectured critical end point.

In Fig. 4 we show the net quark and isovector susceptibilities  $\chi_q$  and  $\chi_I$  along the phase boundary, given in Fig. 2. The position of the TCP is signaled by the singularity of the net quark susceptibility  $\chi_q$ . The corresponding non-monotonic behavior of the fluctuations with increasing beam energy may give rise to observable effects in heavy-ion collisions [4] <sup>#4</sup>. We find that the critical region, where the fluctuations are dominated by the singularity, corresponds to a window  $\Delta T \simeq 30$  MeV and  $\Delta \mu \simeq 10$  MeV around the TCP. In the absence of a TCP, the net quark susceptibility would be a monotonic function of  $T$  along the phase boundary, as illustrated by the dashed-dotted line in Fig. 4. We note that the qualitative behavior of the susceptibility is consistent with the results of Landau theory discussed above. First, the discontinuity across the phase boundary vanishes at  $\mu_q = 0$ . Second, the singularity of  $\chi_q$  shows up only in the chirally broken phase, while the susceptibility in the symmetric phase is monotonous along the phase boundary and shows no singular behavior.

In nucleus-nucleus collisions a change of the collision energy  $\sqrt{s}$  is correlated with a corresponding change of the temperature and the chemical potential. An increase of  $\sqrt{s}$  results in an increase of the temperature  $T$  and a decrease of the baryon chemical potential  $\mu_q$ . Thus, the critical region around tricritical point/critical end point  $(\Delta T, \Delta \mu)$  can be (approximately) converted to a range of center-of-mass energies in A-A collisions. Assuming for simplicity that the relation of  $T_c$  and  $\sqrt{s}$  is the same as for the chemical freezeout parameters extracted from data [48], we find that  $\Delta T \simeq 30$  MeV corresponds to  $\Delta \sqrt{s} \sim 1$  A-GeV. Consequently, this crude estimate implies that in order to observe effects of critical fluctuations in A-A collisions one would need to measure an excitation function with an energy step  $\Delta \sqrt{s}$  smaller than 1 A-GeV.

---

<sup>#4</sup> A similar non-monotonic behavior appears in any observable, directly related to the net quark number density-density correlator. Thus, measurements of the corresponding non-monotonic structure in the baryon number or electric charge density, net-proton number density or in the mean transverse momentum would be excellent experimental probes of the critical end point in the QCD phase diagram.

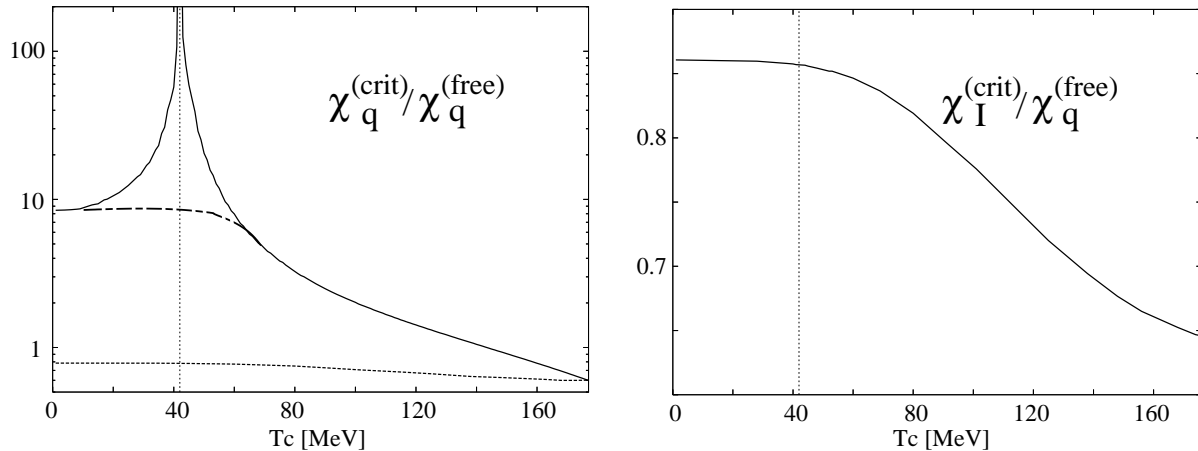


FIG. 4: The quark number (left) and isovector (right) susceptibilities  $\chi_q$  and  $\chi_I$  as functions of the temperature along the phase boundary. In the left-hand figure the solid (dashed) line denotes  $\chi_q$  in the chirally broken (symmetric) phase. The vertical dotted-line indicates the position of the tricritical point TCP. The calculations were done in the chiral limit in an isospin symmetric system with the vector coupling constant  $G_V^{(S)} = 0.3 G_S$ .

In the calculation of the critical properties we have employed the mean-field approximation, which in general does not yield the correct critical exponents [49]. We note however that the non-mean-field critical behavior is suppressed near the TCP, since the quartic coupling  $b(T_{TCP}, \mu_{TCP})$  vanishes [6, 50]. Thus, the critical exponents of the TCP are close to the mean-field exponents [51] and mean-field theory provides a good description of e.g. the susceptibilities near the TCP. Since the physical quark masses are small, the critical end point is influenced by the tricritical point. Thus, one expects the region near the critical end point, where mean-field theory breaks down, to be relatively small [6].

Both at the TCP and at the critical end point the quark-number susceptibility  $\chi_q$  diverges. However, the critical exponents differ. The mean-field exponents of the TCP and the CEP can be obtained from Landau theory. As discussed in Appendix C, the critical exponent for paths approaching the TCP asymptotically tangential to the phase boundary, the susceptibility diverges with the critical exponent  $\gamma_q = 1$ . Approaching the TCP along the first-order transition, the pre-factor is twice as large as along the O(4) critical line. For other paths the critical exponent is  $\gamma_q = \frac{1}{2}$ . At the O(4) critical line, the susceptibility remains finite. The corresponding critical exponent of the O(4) universality class is  $\alpha \simeq -0.2$ , while in the NJL model we obtain the mean-field value for this critical exponent,  $\alpha = 0$ . Finally we mention that for non-zero quark mass, at the critical endpoint, the mean-field critical exponent along a path not tangential to the phase boundary is  $2/3$ , while along the phase boundary it remains equal to unity [6]. When fluctuations are included, the first exponent is renormalized to that of the 3D Ising model universality class [51], i.e.  $\epsilon = 0.78$ .

In Fig. 5 we illustrate the critical behavior near the O(4) critical line and at the TCP. The dependence on the reduced temperature  $t$  is consistent with the exponents and relative pre-factors obtained in Landau theory. The different behavior of the quark number susceptibility at the critical end point and at the O(4) critical line can be traced to the critical behavior of the dynamical quark mass. In Appendix C we compute the mean-field exponents for the dynamical quark mass in Landau theory. At the O(4) critical line  $M^2 \sim |t|$ , while at the TCP  $M^2 \sim |t|^{\frac{1}{2}}$ . The scaling of  $M^2$  obtained in the NJL model are consistent with this, as shown in the right panel of Fig. 5.

Furthermore, in Fig. 6 we also show the “critical” region, where the susceptibility exceeds the free one by more than an order of magnitude<sup>#5</sup>. The different critical exponents along the phase boundary and perpendicular to it are reflected in the shape of the critical region. It is elongated along the phase boundary, where the singularity is strongest.

In heavy ion collision an additional complication to explore and map the QCD phase diagram experimentally appears due to expansion dynamics, finite system size and secondary hadronic rescattering in a medium. All these effects can dilute observation of the critical fluctuations along the chiral phase transition line [52].

<sup>#5</sup> By “critical” region we mean here the region where the susceptibility is large due to fluctuations, not the region of no-mean-field critical behavior.

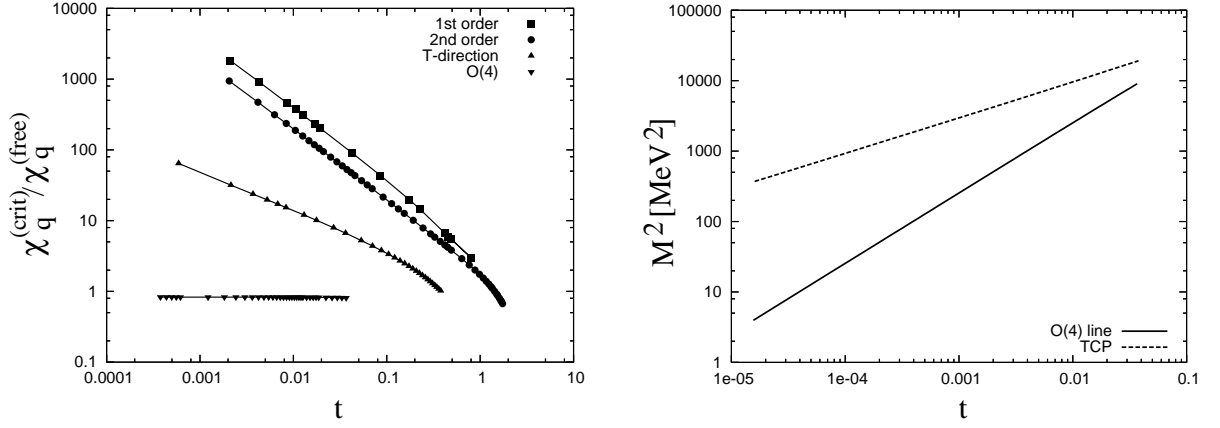


FIG. 5: The quark number susceptibility near the tricritical point (left) and the scaling of the quark mass as the TCP and O(4) critical line is approached (right). At the TCP the reduced temperature is given by  $t = |T - T_{TCP}|/T_{TCP}$ , while at the O(4) line it equals  $t = |T - T_c|/T_c$ .

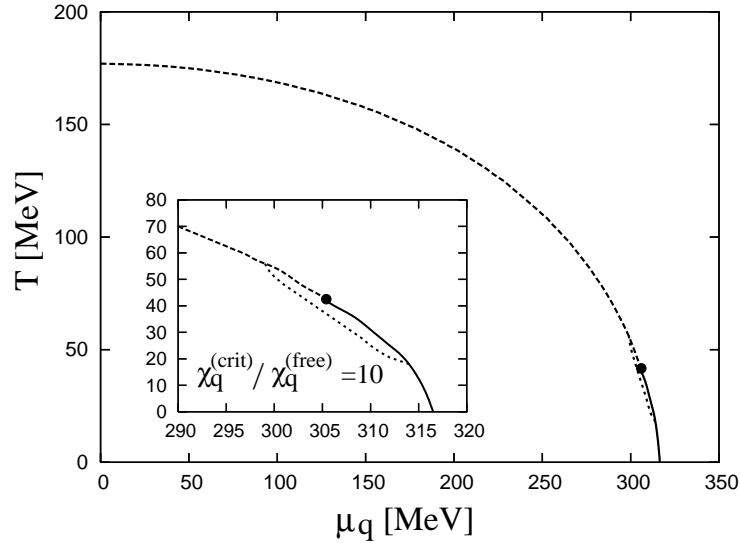


FIG. 6: The “critical” region in the  $T - \mu$  plane obtained in the NJL model. Within this region the susceptibility is enhanced by an order of magnitude compared to the free one.

An interesting observable that characterizes thermal fluctuations related with isospin conservation is the isovector susceptibility  $\chi_I$  defined in Eq. (3.1). The NJL model results for  $\chi_I$  in the isospin symmetric system are shown in Fig. 7 as a function of  $T$  for different  $\mu_q$ . The isovector fluctuations, contrary to net quark fluctuations, are neither singular nor discontinuous at the chiral phase transition for finite chemical potential. As shown in Fig. 4, we find a rather smooth increase of  $\chi_I$  with increasing  $\mu_q$  along phase boundary line. At the TCP where the net quark number susceptibility diverges,  $\chi_I$  remains finite. The non-singular behavior of  $\chi_I$  at the TCP is consistent with the observation that there is no mixing between isovector excitations and the isoscalar sigma field due to  $SU(2)_V$  isospin symmetry[53]. Also recent LGT results [26] show a smooth change of the isovector fluctuations around the deconfinement transition and a fairly weak dependence of  $\chi_I$  on the quark chemical potential  $\mu_q$ .

The net quark number  $\chi_q$  and the isovector  $\chi_I$  susceptibilities are related with fluctuations of the electric charge  $\chi_Q$

$$\chi_Q = \frac{1}{36}\chi_q + \frac{1}{4}\chi_I + \frac{1}{6} \frac{\partial^2 P}{\partial \mu_q \partial \mu_I}. \quad (3.11)$$

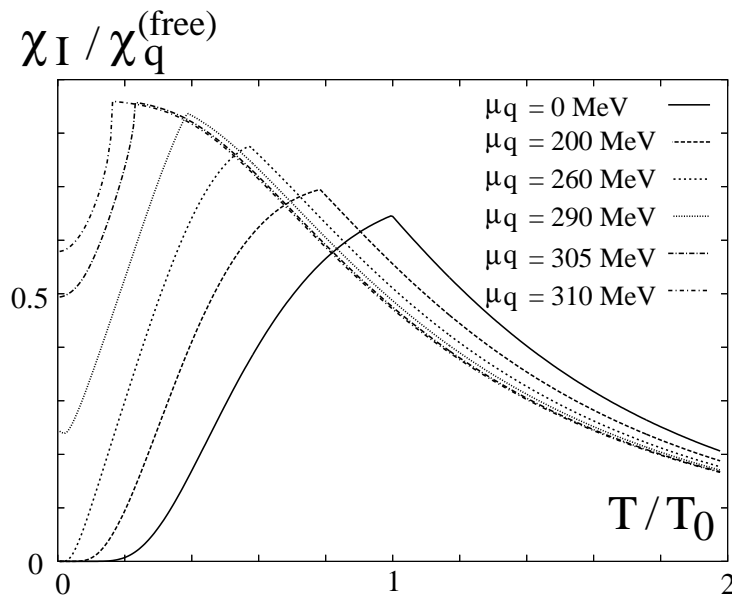


FIG. 7: The isovector susceptibilities  $\chi_I$  for different values of net quark chemical potentials  $\mu_q$  as a function of  $T/T_0$  in the chiral limit. The calculations correspond to isospin symmetric system and the vector coupling constant  $G_V^{(S)} = 0.3 G_S$ .

Here  $P$  is the thermodynamic pressure. For isospin symmetric system the last term in Eq. (3.11) vanishes. Hence in this case all relevant susceptibilities are linearly dependent. Clearly, since  $\chi_I$  is finite at the TCP, the electric charge fluctuations  $\chi_Q$  diverge with the same critical behavior as  $\chi_q$ . However, at finite  $\mu_I$  the properties of  $\chi_I$  at the chiral phase transition in general and at the TCP in particular, change. At non-vanishing  $\mu_I$ , the  $SU(2)_V$  symmetry is explicitly broken. Thus, the isoscalar sigma field mixes with the isospin density [53]. Consequently, the isovector susceptibility exhibits a similar structure as  $\chi_q$ , with a singularity at the TCP. Furthermore, at finite  $\mu_I$  and away from TCP one expects a peak in  $\chi_I$  at the chiral phase transition. This is due to the exponential dependence of the susceptibility on  $\mu_I$  for massive constituent quarks in the broken phase and the power-law dependence in the chirally symmetric phase where the quarks are massless.

### 3.2. Model parameter dependence of quark susceptibilities in the chiral limit

In the previous section, where we considered the net quark and isovector susceptibilities, the coupling constants of the effective interaction between constituent quarks were fixed by requiring that the model reproduces vacuum observables. In the following we discuss the influence of changes in the model parameters on the critical properties of the quark flavor fluctuations. We also present results for the flavor diagonal and off-diagonal susceptibilities  $\chi_{uu}$  and  $\chi_{ud}$  and discuss their properties.

In Fig. 8 the temperature dependence of the flavor diagonal susceptibility  $\chi_{uu}$  is shown for several values of the quark chemical potential for two choices of the vector couplings  $G_V^{(V)}$ . The susceptibility is normalized to the free one  $\chi_{uu}^{(\text{free})}$ , which is defined by  $\chi_{uu}^{(\text{free})} = \chi_q^{(\text{free})}/N_f$ .

At vanishing chemical potential there are generic features in the temperature dependence of the quark flavor susceptibilities. Consider the net quark  $\chi_q$ , the isovector  $\chi_I$  and flavor diagonal  $\chi_{uu}$  susceptibilities shown in Figs. 3, 7 and 8. Clearly all these susceptibilities are strongly enhanced near the chiral phase transition point  $T_0$ , while above  $T_0$  the fluctuations are suppressed. The increase of the quark susceptibilities with temperature seen in the broken symmetry phase reflects a decrease of the dynamical quark mass as the chiral transition is approached. Consequently, the enhancement of the quark fluctuations is, in this model, mainly due to the amplification of the Boltzmann factor  $\exp(-M/T)$  as the constituent quark mass is reduced. The suppression of  $\chi_q$ ,  $\chi_I$  and  $\chi_{uu}$  above  $T_c$  is due to the finite momentum cut-off of the NJL model. Indeed, the flavor-diagonal susceptibility  $\chi_{uu}$  in an ideal massless quark

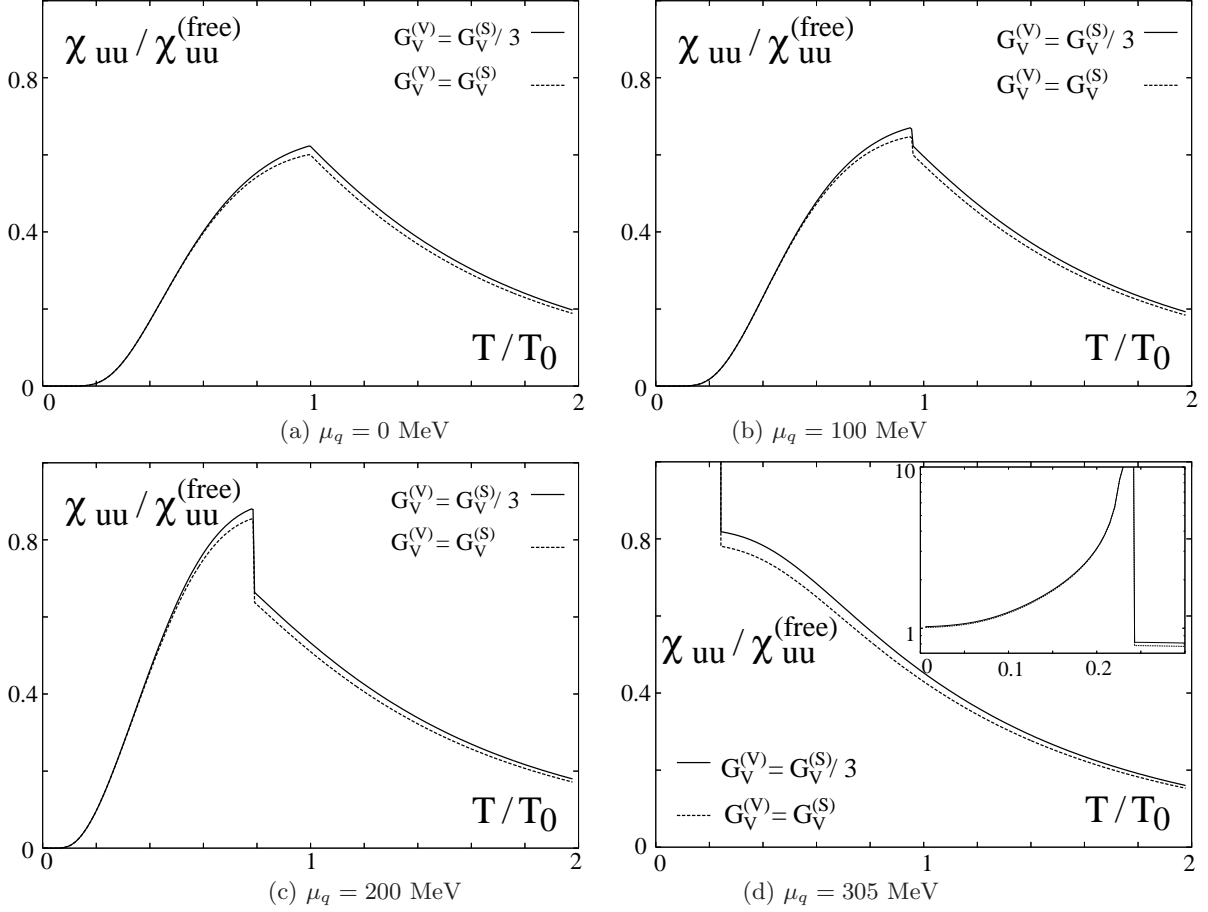


FIG. 8: The diagonal  $\chi_{uu}$  susceptibility in an isospin symmetric system for  $\mu_q = 0, 100, 200$  and  $305$  MeV in the chiral limit normalized to  $\chi_{uu}^{(free)}$  as a function of  $T/T_0$ . The calculations correspond to the vector coupling constants  $G_V^{(V)} = 0.3 G_S$  and  $G_V^{(V)}/G_V^{(S)} = 1/3$  and  $1$ .

gas with momentum cut-off  $\Lambda$  is given by

$$\begin{aligned} \chi_{uu}^{(free)}/T^2 &= \frac{12}{T^3} \int_0^\Lambda \frac{d^3p}{(2\pi)^3} \frac{e^{p/T}}{(1+e^{p/T})^2} \\ &\simeq 1 - \frac{12}{\pi^2} e^{-\Lambda/T} \left(1 + \frac{\Lambda}{T} + \frac{1}{2} \frac{\Lambda^2}{T^2}\right) + \dots, \end{aligned} \quad (3.12)$$

where the ellipsis in the second stands for terms that are exponentially suppressed for  $T < \Lambda$ . For  $\Lambda \rightarrow \infty$  one obtains the ideal gas result  $\chi_{uu}^{(free)}/T^2 = 1$ , while for finite  $\Lambda$  the fluctuation are suppressed. At low temperature  $T \ll \Lambda$ , the correction terms in Eq. (3.12) are negligible, and  $\chi$  is independent of  $\Lambda$ . However, for temperatures on the order of  $\Lambda$  there is a strong dependence on the cut-off. With increasing temperature the suppression of  $\chi_q$ ,  $\chi_I$  and  $\chi_{uu}$  grows stronger, as seen in Fig. 10. As seen in Fig. 10 this holds also for  $\chi_q$  and  $\chi_I$ . However, the cutoff dependence of  $\chi_{ud}$  is different. Here, since  $\chi_{ud} \propto \chi_q - \chi_I$ , the cut-off dependence of  $\chi_q$  and  $\chi_I$  partly cancel. Thus, the trend above and below  $T_0$  is different. At low temperatures the magnitude of  $\chi_{ud}$  is reduced and at high temperatures enhanced with increasing  $\Lambda$ . We remind the reader that both parameter sets (a) and (b) yield the same transition temperature  $T_0 = 177$  MeV at  $\mu_q = 0$  (see Table 1).

In Figs. 8 and 9 we also show the dependence of  $\chi_{uu}$  and  $\chi_{ud}$  on the choice of vector couplings. The dependence of  $\chi_{uu}$  on  $G_V^{(V)}$  is fairly weak, as seen in Fig. 8. This is because in isospin symmetric matter ( $\mu_I = 0$ )  $G_V^{(V)}$  contributes only to  $\chi_I$ , which is much smaller than  $\chi_q$  (cf. Fig. 4). Consequently,  $\chi_{uu}$  is essentially determined by  $\chi_q$ , which depends on  $G_S$  and  $G_V^{(S)}$ .

A comparison of Fig. 8 and 9 shows that the off-diagonal susceptibility  $\chi_{ud}$  is much smaller in magnitude than  $\chi_{uu}$ .

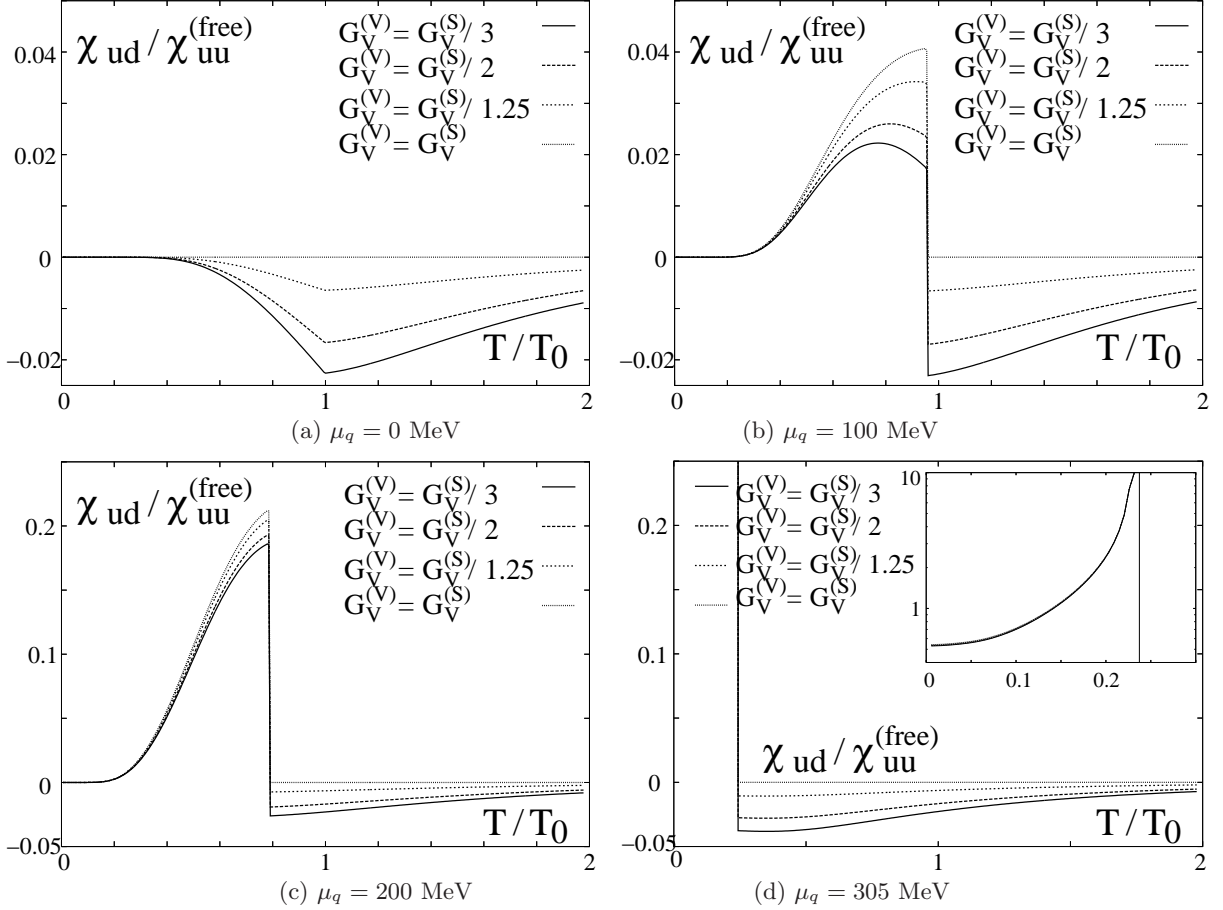


FIG. 9: The off-diagonal  $\chi_{ud}$  susceptibility in an isospin symmetric system for  $\mu_q = 0, 100, 200$  and  $305$  MeV in the chiral limit normalized to  $\chi_{uu}^{(free)}$  as a function of  $T/T_0$ . The calculations correspond to the vector coupling constants  $G_V^{(S)} = 0.3 G_S$  and  $G_V^{(V)}/G_V^{(S)} = 1/3$  and  $1$ .

Still,  $\chi_{ud}$  is an interesting observable, which may be used to identify the transition point. This is particularly the case at finite  $\mu_q$  where the off-diagonal susceptibility is changing sign when crossing the critical temperature. This behavior is consistent with the recent LGT findings which shows negative values of  $\chi_{ud}$  below and above deconfinement for  $\mu_q = 0$ . At finite  $\mu_q$  and at  $T = T_c$  the LGT results show [26] an abrupt change of  $\chi_{ud}$  from negative to positive value. At the tricritical point,  $\chi_{ud}$ , being proportional to  $\chi_q - \chi_I$ , diverges as  $\chi_q$  (see Fig. 9 (d)). Also seen in Fig. 9 is a rather strong variation of  $\chi_{ud}$  with the strength of  $G_V^{(S)}/G_V^{(V)}$  ratio. Above the chiral phase transition,  $\chi_q$  and  $\chi_I$  are equal for  $G_V^{(S)} = G_V^{(V)}$ . Hence, the fact that in LGT  $\chi_{ud}$  is very small above  $T_0$ , may be interpreted as a signature of the universality of the isosclar and isovector current-current interaction in the chirally restored phase. For  $\mu_q = 0$ ,  $\chi_{ud}$  vanishes also in the chirally broken phase if  $G_V^{(S)} = G_V^{(V)}$ . The fact that in LGT  $\chi_{ud}$  is negative in this temperature range, is consistent with  $G_V^{(S)} > G_V^{(V)}$ , as expected for baryons from large  $N_c$  arguments.

### 3.3. Susceptibilities at finite current quark mass

So far, we have computed the susceptibilities in the chiral limit, i.e., using an effective Lagrangian with an exact symmetry, the chiral symmetry. However, the chiral symmetry of the QCD Lagrangian is only approximate due to the finite current quark masses. In the following, we account for the explicit chiral symmetry breaking and explore its influence on the quark number fluctuations. This study could be also interesting from the perspective of recent LGT results [26] where the susceptibilities were calculated for finite and large quark masses.

In Fig. 11 we show results obtained with the NJL model for the flavor diagonal  $\chi_{uu}$  and off-diagonal  $\chi_{ud}$  suscep-



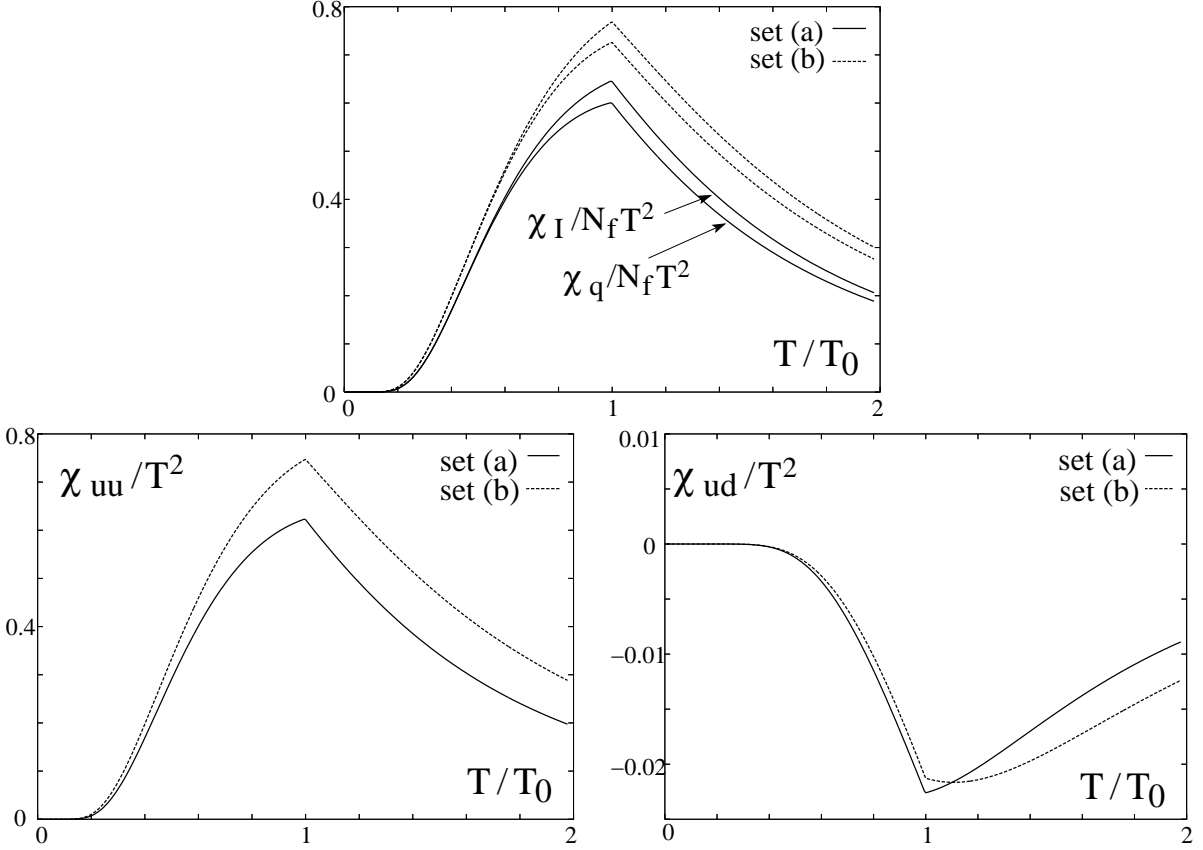


FIG. 10: The susceptibilities for isospin symmetric system in the chiral limit normalized to  $\chi^{(\text{free})}$  at  $\mu_q = 0$  as a function of  $T/T_0$  for  $G_V^{(V)}/G_V^{(S)} = 1/3$ . The solid line corresponds to the parameter set (a) and the dashed line to the set (b) listed in Table I.

tibilities for different values of the current quark mass. These calculations were done both for vanishing and finite chemical potential as well as for several sets of the vector coupling constant.

A comparison of the results for different quark masses clearly shows that  $\chi_{uu}$  exhibits a peak structure at finite temperature, indicating the phase change, for all values of  $m$ . However, at finite  $m$  the  $\chi_{uu}$  is a smooth function everywhere, whereas in the chiral limit it exhibits a non-analytic structure at the phase transition. This behavior indicates that the second order transition at  $m = 0$  is converted into a smooth cross-over at finite  $m$ . The above is even more transparent at finite  $\mu_q$  where the discontinuity of  $\chi_{uu}$  at  $T_c$  disappears at finite quark mass. The behavior of the NJL model at finite  $m$  is in accord with recent LGT finding in 2-flavor QCD, which also shows a cross-over transition at finite quark mass. We note, however, that the second-order transition expected in the NJL model in the chiral limit is still not confirmed by LGT calculations. Some recent results even suggest that in 2-flavor QCD this transition could be weakly first order [54].

With increasing quark mass the peak position of  $\chi_{uu}/T^2$  is shifted towards larger  $T$ , both at vanishing and at finite  $\mu_q$ . The height of the peak also depends on  $m$  and decreases with increasing current quark mass. The shift of the peak position in  $\chi_{uu}$  indicates an increase of the pseudo-critical temperature with increasing quark mass. Such an effect was observed in lattice calculations already some time ago [45]. Also the suppression of quark number fluctuations with increasing quark mass is found in recent LGT calculations both at vanishing and at finite  $\mu_q$ . This suppression is related to an upward shift of the hadronic mass spectrum [31], which leads to a reduction of the number of thermally excited hadrons  $\sim \exp(-M_h/T)$ . The suppression of  $\chi_{uu}$  in the NJL model is of similar origin; the number of thermally excited quarks is cut back by the corresponding increase of the dynamical quark mass. The increase of  $\chi_{uu}$  with  $\mu_q$  seen in Fig. 11 can be understood in terms of the corresponding increase of the thermal factors  $\sim \exp(\mu_q/T)$ . Finally, at large temperatures  $T > T_0$  the NJL model shows a very weak dependence of the susceptibilities on the current quark mass independently of the value of  $\mu_q$ . In lattice calculations of QCD the  $m_q$ -dependence of thermodynamic quantities was also found to be weak for  $m_q/T < 1$ .

The influence of a non-zero current quark mass on the off-diagonal susceptibility  $\chi_{ud}$  for different values of  $\mu_q$  and

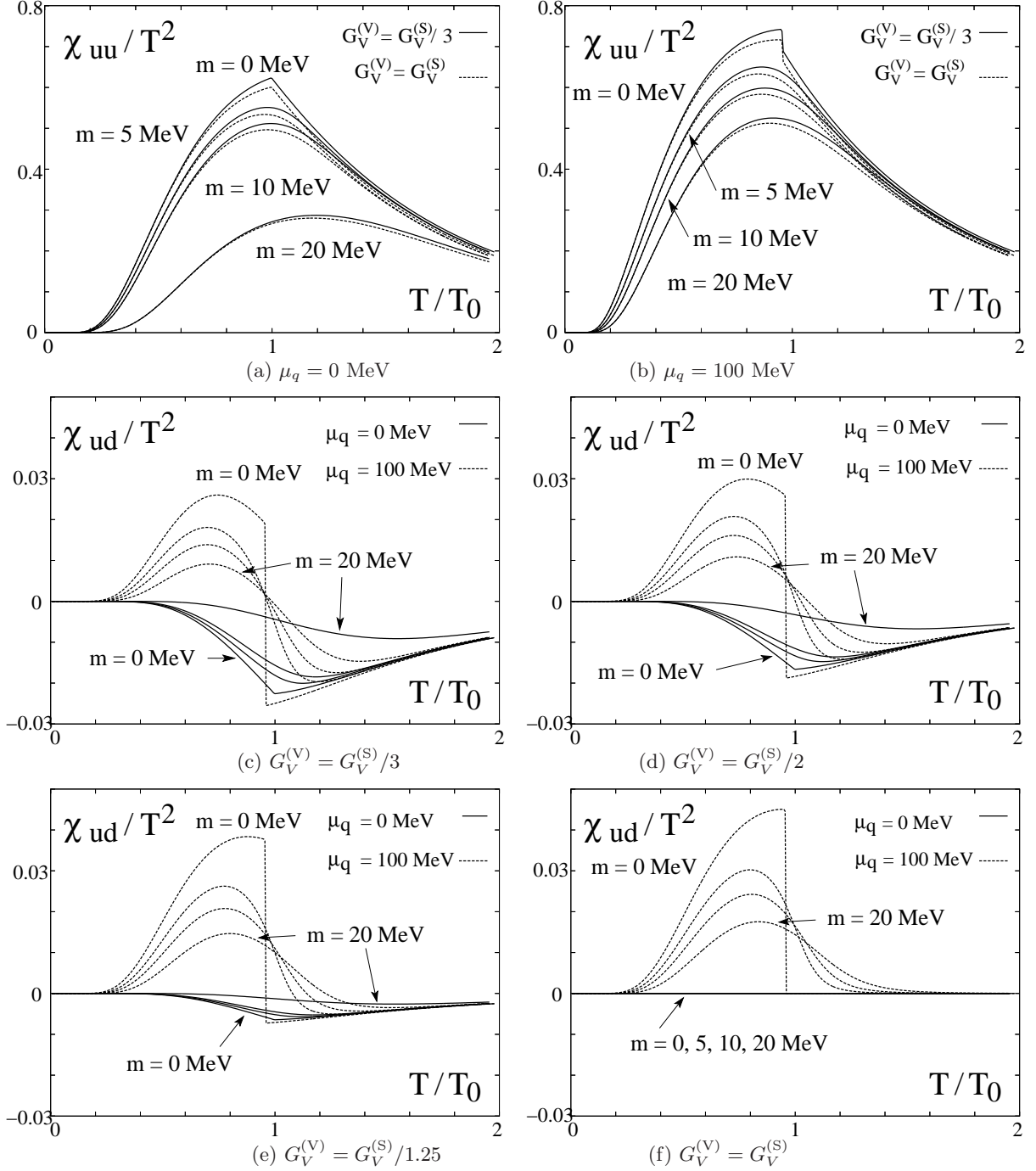


FIG. 11: The diagonal and off-diagonal susceptibilities normalized to  $T^2$  for different values of the current quark mass as a function of  $T/T_0$ . For the pseudo-critical temperature for  $m = 5$  MeV we find  $T_0 = 179$  MeV. The results correspond to  $\mu_q = 0$  and 100 MeV and the vector coupling constants  $G_V^{(S)} = 0.3 G_S$  with  $G_V^{(V)}/G_V^{(S)} = 1/3$  and 1.

vector couplings is illustrated in Figs. 11 (c)-(f). For  $\mu_q = 0$  and  $G_V^{(V)}/G_V^{(S)} < 1$ ,  $\chi_{ud}$  is finite and negative for all  $T$ , and approaches zero for large temperatures. A similar behavior is observed in 2-flavor QCD on the lattice [26]. When  $G_V^{(V)}/G_V^{(S)}$  is increased towards unity,  $\chi_{ud}$  approaches zero at all temperatures. At finite  $\mu_q$ , the temperature dependence of  $\chi_{ud}$  changes qualitatively. Below  $T_c$  it is negative, while above  $T_c$  it is positive, in qualitative agreement with the results of LGT calculations [26]. The off-diagonal susceptibility  $\chi_{ud}$  is finite near the pseudo-critical transition for all values of  $m$ .

When discussing the influence of the model parameters on quark number susceptibilities we have allowed for variations of the parameters. However, we have not considered a possible  $T$  and  $\tilde{\mu}$  dependence of  $G_S, G_V$  and  $\Lambda$ . It was recently argued that such a dependence is important for a quantitative comparison of NJL model results with LGT findings [55]. However, so far systematic calculations of the variation of these parameters with temperature and chemical potential are lacking. A possible temperature dependence of these parameters was obtained phenomenologically by comparing some observables with lattice results.

#### 4. SUMMARY AND CONCLUSIONS

We have discussed the properties of quark number fluctuations within the framework of the Nambu–Jona-Lasinio (NJL) model. The model was formulated at finite temperature and chemical potentials for baryon number and isospin. In a mean field approach, we have shown how the fluctuations of different quark flavors are changing across the phase boundary. Such a study is of interest from the perspective of both heavy ion phenomenology and lattice gauge theory. In the first case we have explored the non-monotonic structure of net quark, diagonal and off-diagonal susceptibilities along the phase transition line. We have also discussed the critical region around the tricritical point in the context of heavy ion phenomenology.

The results on different quark susceptibilities at finite quark mass are in qualitative agreement with recent findings on the lattice. Our study may give some insight into how lattice results may change when one approaches the chiral limit at vanishing and at large baryon chemical potential. This expectation is supported by the fact that the NJL model exhibits the same critical properties as one expects for QCD.

Obviously, the NJL model differs substantially from QCD. This model does not contain all relevant hadronic degrees of freedom, which in QCD contribute substantially to the quark number susceptibilities. Moreover, the phase-space of dynamical quarks is suppressed by the ultraviolet cut-off. Consequently, the perturbative regime of QCD at high temperature and density is not reproduced by this model. Nevertheless, features of the quark number susceptibilities that probe the restoration of chiral symmetry can be studied in some detail in NJL model calculations. In particular the change in the behavior of the quark fluctuations near the critical point can be interpreted as an effective change of the vector interaction associated with the chiral phase transition.

#### Acknowledgments

We acknowledge interesting discussions with F. Karsch, S. Leupold, and J. Wambach. C.S. also acknowledges fruitful discussions with H. Fujii and B. J. Schaefer. The work of B.F. and C.S. were supported in part by the Virtual Institute of the Helmholtz Association under the grant No. VH-VI-041. K.R. acknowledges partial support of the Gesellschaft für Schwerionenforschung (GSI) and KBN under grant 2P03 (06925).

#### APPENDIX A: ANALYTICAL RESULTS FOR THE PHASE BOUNDARY

For massless quarks, the gap equation (2.13) at the chiral transition can be obtained in closed form. At the second order transition, the gap equation has a non-trivial solution at  $M = 0$ , i.e.

$$1 = 4G_S N_c \sum_f \int \frac{d^3p}{(2\pi)^3} \frac{1}{p} \left[ 1 - n_f^{(+)}(\vec{p}, T, \tilde{\mu}_f) - n_f^{(-)}(\vec{p}, T, \tilde{\mu}_f) \right] \quad (\text{A.1})$$

is satisfied. After some rearrangement one finds for  $\tilde{\mu}_u = \tilde{\mu}_d = \tilde{\mu}$

$$\frac{\Lambda^2}{2} - \frac{\pi^2}{4G_S N_c} = I(T, \tilde{\mu}), \quad (\text{A.2})$$

where the quadratically divergent term on the left hand side is due to the vacuum loop and  $I(T, \tilde{\mu})$  to the thermal loops. The explicit form of the latter is given by

$$\begin{aligned} I(T, \mu) &= \int_0^\Lambda dpp \left( \frac{1}{e^{\beta(p-\mu)} + 1} + \frac{1}{e^{\beta(p+\mu)} + 1} \right) \\ &= \frac{\pi^2 T^2}{6} + \frac{\mu^2}{2} + T^2 \left[ \text{L}_2(-e^{-\beta(\mu+\Lambda)}) + \text{L}_2(-e^{\beta(\mu-\Lambda)}) \right] \\ &\quad - T\Lambda \log \left[ (1 + e^{-\beta(\mu+\Lambda)})(1 + e^{\beta(\mu-\Lambda)}) \right], \end{aligned} \quad (\text{A.3})$$

where  $L_2[z] = \sum_{n=1}^{\infty} z^n/n^2$  is Euler's dilogarithm [56].

We now use (A.3) to explore the dependence of the phase boundary on the cut off  $\Lambda$ . A general variation of (A.2) yields

$$\Lambda\delta\Lambda + \frac{\pi^2}{4G_S^2 N_c} \delta G_s = \frac{\partial I}{\partial \Lambda} \delta\Lambda + \frac{\partial I}{\partial T} \delta T + \frac{\partial I}{\partial \mu} \delta\mu. \quad (\text{A.4})$$

At  $\mu = 0$ ,  $\partial I/\partial \mu = 0$  by symmetry and

$$\frac{\partial I}{\partial \Lambda} = \frac{2}{e^{\beta\Lambda} + 1} \Lambda. \quad (\text{A.5})$$

Thus, the requirement that the critical temperature at vanishing net quark density remains fixed, as in the right panel of Fig. 2, implies the following relation between the cut off  $\Lambda$  and the coupling constant  $G_S$

$$\Lambda\delta\Lambda + \frac{\pi^2}{4G_S^2 N_c} \delta G_s = \frac{2}{e^{\beta\Lambda} + 1} \Lambda\delta\Lambda. \quad (\text{A.6})$$

Assuming that the transition is second order everywhere, the shift of the critical value of the chemical potential at  $T = 0$  is given by

$$\delta\mu = \frac{1}{\mu} \left( \Lambda\delta\Lambda + \frac{\pi^2}{4G_S^2 N_c} \delta G_s \right) = \frac{2}{e^{\Lambda/T} + 1} \frac{\Lambda}{\mu} \delta\Lambda. \quad (\text{A.7})$$

This relation, which remains approximately valid also when the transition is weakly first order, provides a quantitative interpretation of the shift of the phase boundary shown in the right panel of Fig. 2.

Using the fact that for reasonable parameter choices,  $e^{\beta(\pm\mu-\Lambda)} \ll 1$  along the phase boundary, useful approximative expressions may be obtained for  $I(T, \mu)$ . Retaining the first two terms in the expansions of the dilogarithms and the logarithm in (A.3), we find

$$\begin{aligned} I(T, \mu) &= \frac{\pi^2 T^2}{6} + \frac{\mu^2}{2} - T(T + \Lambda) \left( e^{\beta(\mu-\Lambda)} + e^{-\beta(\mu+\Lambda)} \right) \\ &\quad + \frac{1}{4} T(T + 2\Lambda) \left( e^{2\beta(\mu-\Lambda)} + e^{-2\beta(\mu+\Lambda)} \right). \end{aligned} \quad (\text{A.8})$$

Within this approximation, one finds the critical temperature at  $\mu = 0$  with an accuracy of  $\sim 10^{-5}$ . For non-zero  $\mu$  the approximation becomes increasingly better, since the  $\Lambda$ -dependent terms drop out for  $T \rightarrow 0$ . We note in passing that a solution of Eqn. (A.2) is possible only if the left hand side is positive, i.e., for  $G_S \Lambda^2 > \pi^2/(2N_c) \simeq 1.64$ . For smaller values of the scalar coupling constant, chiral symmetry is never broken.

## APPENDIX B: DERIVATIVES OF EFFECTIVE CONDENSATES

In this appendix, we summarized derivatives of the dynamical masses  $M_f$  and the shifted chemical potentials  $\tilde{\mu}_f$ . These results are obtained from the gap equations (2.13)- (2.15) by taking derivatives with respect to  $\mu_q$  and  $\mu_I$  as

$$\begin{aligned} \frac{\partial M_f}{\partial \mu_{q,I}} &= \frac{\partial M_f}{\partial \mu_{q,I}} A_f + \frac{\partial M_{f'}}{\partial \mu_{q,I}} A_{f'} + \frac{\partial \tilde{\mu}_f}{\partial \mu_{q,I}} B_f + \frac{\partial \tilde{\mu}_{f'}}{\partial \mu_{q,I}} B_{f'}, \\ 1 &= \frac{\partial \tilde{\mu}_u}{\partial \mu_{q,I}} + \frac{\partial M_u}{\partial \mu_{q,I}} C_u^{(S)} + \frac{\partial M_u}{\partial \mu_{q,I}} C_u^{(V)} + \frac{\partial M_d}{\partial \mu_{q,I}} C_d^{(S)} - \frac{\partial M_d}{\partial \mu_{q,I}} C_d^{(V)} \\ &\quad + \frac{\partial \tilde{\mu}_u}{\partial \mu_{q,I}} D_u^{(S)} + \frac{\partial \tilde{\mu}_u}{\partial \mu_{q,I}} D_u^{(V)} + \frac{\partial \tilde{\mu}_d}{\partial \mu_{q,I}} D_d^{(S)} - \frac{\partial \tilde{\mu}_d}{\partial \mu_{q,I}} D_d^{(V)}, \\ \pm 1 &= \frac{\partial \tilde{\mu}_d}{\partial \mu_{q,I}} + \frac{\partial M_u}{\partial \mu_{q,I}} C_u^{(S)} - \frac{\partial M_u}{\partial \mu_{q,I}} C_u^{(V)} + \frac{\partial M_d}{\partial \mu_{q,I}} C_d^{(S)} + \frac{\partial M_d}{\partial \mu_{q,I}} C_d^{(V)} \\ &\quad + \frac{\partial \tilde{\mu}_u}{\partial \mu_{q,I}} D_u^{(S)} - \frac{\partial \tilde{\mu}_u}{\partial \mu_{q,I}} D_u^{(V)} + \frac{\partial \tilde{\mu}_d}{\partial \mu_{q,I}} D_d^{(S)} + \frac{\partial \tilde{\mu}_d}{\partial \mu_{q,I}} D_d^{(V)}, \end{aligned} \quad (\text{B.1})$$

where  $f \neq f' \in \{u, d\}$  and the functions  $A_f, B_f, C_f^{(S,V)}$  and  $D_f^{(S,V)}$  are defined by

$$\begin{aligned}
A_f &= 4G_S N_c \int \frac{d^3 p}{(2\pi)^3} \frac{1}{E_f} \left[ \left( 1 - \frac{M_f^2}{E_f^2} \right) (1 - n_f^{(+)} - n_f^{(-)}) \right. \\
&\quad \left. + \frac{M_f^2}{TE_f} \left[ n_f^{(+)} (1 - n_f^{(+)} + n_f^{(-)} (1 - n_f^{(-)})) \right] \right], \\
B_f &= 4G_S N_c \int \frac{d^3 p}{(2\pi)^3} \frac{-M_f}{TE_f} \left[ n_f^{(+)} (1 - n_f^{(+)} - n_f^{(-)} (1 - n_f^{(-)})) \right], \\
C_f^{(S,V)} &= 4G_V^{(S,V)} N_c \int \frac{d^3 p}{(2\pi)^3} \frac{-M_f}{TE_f} \left[ n_f^{(+)} (1 - n_f^{(+)} - n_f^{(-)} (1 - n_f^{(-)})) \right], \\
D_f^{(S,V)} &= 4G_V^{(S,V)} N_c \int \frac{d^3 p}{(2\pi)^3} \frac{1}{T} \left[ n_f^{(+)} (1 - n_f^{(+)} + n_f^{(-)} (1 - n_f^{(-)})) \right].
\end{aligned} \tag{B.2}$$

Solving Eq. (B.1) one gets,

$$\begin{aligned}
\frac{\partial M_u}{\partial \mu_{q,I}} &= \left[ B_u (1 + 2D_d^{(V,S)}) \pm B_d (1 + 2D_u^{(V,S)}) \right] / F, \\
\frac{\partial M_d}{\partial \mu_{q,I}} &= \frac{\partial M_u}{\partial \mu_{q,I}} \\
\frac{\partial \tilde{\mu}_u}{\partial \mu_{q,I}} &= \left[ 1 - (A_u + A_d) (1 + 2D_d^{(V,S)}) \mp 2B_d (C_u^{(V,S)} \mp C_d^{(V,S)}) + 2D_d^{(V,S)} \right] / F, \\
\frac{\partial \tilde{\mu}_d}{\partial \mu_{q,I}} &= \pm \left[ 1 - (A_u + A_d) (1 + 2D_u^{(V,S)}) + 2B_u (C_u^{(V,S)} \mp C_d^{(V,S)}) + 2D_u^{(V,S)} \right] / F,
\end{aligned} \tag{B.3}$$

with the function  $F$  expressed by

$$\begin{aligned}
F &= 1 - (A_u + A_d) \left[ 1 + D_u^{(S)} (1 + 2D_d^{(V)}) + D_u^{(V)} (1 + 2D_d^{(S)}) + D_d^{(S)} + D_d^{(V)} \right] \\
&\quad + B_u \left[ C_u^{(S)} + C_d^{(S)} + C_u^{(V)} - C_d^{(V)} \right] + B_d \left[ C_u^{(S)} + C_d^{(S)} - C_u^{(V)} + C_d^{(V)} \right] \\
&\quad + 2 \left[ B_u D_d^{(S)} - B_d D_u^{(S)} \right] \left[ C_u^{(V)} - C_d^{(V)} \right] + 2 \left[ B_u D_d^{(V)} + B_d D_u^{(V)} \right] \left[ C_u^{(S)} + C_d^{(S)} \right] \\
&\quad + D_u^{(S)} \left[ 1 + 2D_d^{(V)} \right] + D_d^{(S)} \left[ 1 + 2D_u^{(V)} \right] + D_u^{(V)} + D_d^{(V)}.
\end{aligned} \tag{B.4}$$

The  $\chi_q$  and  $\chi_I$  susceptibilities are obtained by substituting Eq. (B.3) into Eqs. (3.2) and (3.3).

### APPENDIX C: CRITICAL EXPONENTS IN LANDAU THEORY

In this appendix we compute the mean-field critical exponents of the TCP in Landau theory. Since the fourth order term  $b(T, \mu_q)$  in (3.6) vanishes at the TCP, it is necessary to include a sixth-order term in the expansion of the thermodynamic potential

$$\omega(T, \mu_q, M) \simeq \omega_0(T, \mu_q) + \frac{1}{2} a(T, \mu_q) M^2 + \frac{1}{4} b(T, \mu_q) M^4 + \frac{1}{6} c M^6, \tag{C.1}$$

where  $M$  is the dynamical quark mass. We assume that  $c > 0$  and neglect its dependence on the temperature and chemical potential. At the TCP the coefficients  $a$  and  $b$  both vanish. Close to the TCP we retain the leading terms,

$$\begin{aligned}
a(T, \mu) &= A(T - T_{TCP}) + B(\mu - \mu_{TCP}) \\
b(T, \mu) &= C(T - T_{TCP}) + D(\mu - \mu_{TCP}).
\end{aligned} \tag{C.2}$$

Along the second order phase boundary, the coefficient  $a$  vanishes, while at the first order transition  $a > 0$  and  $b < 0$ . The dynamical mass is determined by minimizing the thermodynamic potential. The solutions of the gap equation

$$\frac{\partial \omega}{\partial M} = M(a + bM^2 + cM^4) = 0 \tag{C.3}$$

are given by  $M = 0$  and  $M^2 = -\frac{b}{2c} \pm \frac{1}{2c}\sqrt{b^2 - 4ac}$ . The quark number susceptibility is given by

$$\chi_q = -\frac{\partial^2 \omega}{\partial \mu_q^2} = \chi_0 - \frac{1}{2} (B + DM^2) \frac{\partial M^2}{\partial \mu_q}. \quad (\text{C.4})$$

As the TCP is approached,  $a, b$  and  $M \rightarrow 0$ . Thus, the singular part of the susceptibility is given by

$$\chi_q^{sing} = \frac{1}{2} \frac{B^2}{\sqrt{b^2 - 4ac}}. \quad (\text{C.5})$$

When the TCP is approached along the second order phase boundary,  $a = 0$ . Consequently  $\chi_q^{sing} = B^2/2|b| \sim |\mu_q - \mu_{TCP}|^{-1}$ . In order to compute the critical exponent along the first order transition, we must first determine the relation between  $a, b$  and  $c$  along this path. At the first order transition there are three degenerate minima of the thermodynamic potential, one at  $M = 0$  corresponding to the symmetric phase, and two at finite  $M$  corresponding to the two realizations of the broken phase. Thus, we are looking for a solution to the two equations

$$\begin{aligned} aM^2 + \frac{1}{2}bM^4 + \frac{1}{3}cM^6 &= 0 \\ a + bM^2 + cM^4 &= 0, \end{aligned} \quad (\text{C.6})$$

for non-vanishing  $M$ . Such a solution,  $M^2 = -3b/4c$ , exists when the coefficients satisfy the relation  $16ac = 3b^2$ . This relation defines the location of the phase boundary in the  $(T, \mu_q)$  plane. Furthermore, it implies that the first-order phase boundary is asymptotically parallel to the second order one. Using the relation in (C.5), we find  $\chi_q^{sing} = B^2/|b| \sim |\mu_q - \mu_{TCP}|^{-1}$ . Thus, the critical exponent is identical to that along the second order line, but the pre-factor is twice as large. If the TCP is approached from the broken phase, along any path which is not asymptotically tangential to the phase boundary at the TCP,  $b^2 \ll 4ac$  for points close to the TCP. This implies that the critical exponent is different, namely  $\chi_q^{sing} = B^2/4\sqrt{ac} \sim |\mu_q - \mu_{TCP}|^{-\frac{1}{2}}$ .

Finally, we explore the scaling behavior of the dynamical quark mass near the O(4) critical line and at the tricritical point. As discussed in the text, this behavior determines the critical properties of the quark number susceptibility. The non-trivial solution of the gap equation implies that for constant chemical potential  $M^2 \sim a \sim |T_c - T|$  at the O(4) critical line, where  $b \neq 0$ . On the other hand, at the critical end point, where also  $b \rightarrow 0$ ,  $M^2 \sim \sqrt{a} \sim |T_{TCP} - T|^{\frac{1}{2}}$ .

- [1] For a recent review, see e.g., S. Jeon and V. Koch, *Quark Gluon Plasma 3*, R. C. Hwa and X.-N. Wang (Eds.), World Scientific, 430 (2004) and references therein
- [2] T. Kunihiro, Phys. Lett. B **271**, 395 (1991)
- [3] G. E. Brown and M. Rho, Phys. Rept. **269**, 333 (1996)
- [4] M. A. Stephanov, K. Rajagopal and E. V. Shuryak, Phys. Rev. Lett. **81**, 4816 (1998)
- [5] G. E. Brown and M. Rho, Phys. Rept. **363**, 85 (2002)
- [6] Y. Hatta and T. Ikeda, Phys. Rev. D **67**, 014028 (2003)
- [7] H. Fujii, Phys. Rev. D **67**, 094018 (2003)
- [8] D. T. Son and M. A. Stephanov, Phys. Rev. Lett. **88**, 202302 (2002); Phys. Rev. D **66**, 076011 (2002); M. Harada, Y. Kim, M. Rho and C. Sasaki, Nucl. Phys. A **727**, 437 (2003)
- [9] M. Gazdzicki and S. Mrowczynski, Z. Phys. C **54**, 127 (1992); M. Asakawa, U. W. Heinz and B. Muller, Phys. Rev. Lett. **85**, 2072 (2000); S. Jeon and V. Koch, Phys. Rev. Lett. **85**, 2076 (2000); Z. W. Lin and C. M. Ko, Phys. Rev. C **64**, 041901 (2001); E. V. Shuryak and M. A. Stephanov, Phys. Rev. C **63**, 064903 (2001)
- [10] V. L. Eletsky, J. I. Kapusta and R. Venugopalan, Phys. Rev. D **48**, 4398 (1993); M. Prakash, R. Rapp, J. Wambach and I. Zahed, Phys. Rev. C **65**, 034906 (2002)
- [11] Z. Fodor and S. D. Katz, JHEP **0203**, 014 (2002); JHEP **0404**, 050 (2004)
- [12] C. R. Allton, S. Ejiri, S. J. Hands, O. Kaczmarek, F. Karsch, E. Laermann and C. Schmidt, Phys. Rev. D **68**, 014507 (2003); Nucl. Phys. Proc. Suppl. **119**, 538 (2003)
- [13] M. D'Elia and M. P. Lombardo, Phys. Rev. D **67**, 014505 (2003)
- [14] P. de Forcrand and O. Philipsen, Nucl. Phys. B **673**, 170 (2003)
- [15] A. Barducci, R. Casalbuoni, S. De Curtis, R. Gatto and G. Pettini, Phys. Lett. B **231**, 463 (1989)
- [16] S. P. Klevansky, Rev. Mod. Phys. **64** (1992) 649
- [17] M. A. Stephanov, Phys. Rev. Lett. **76**, 4472 (1996); Nucl. Phys. Proc. Suppl. **53**, 469 (1997)
- [18] M. G. Alford, K. Rajagopal and F. Wilczek, Phys. Lett. B **422**, 247 (1998)
- [19] R. Rapp, T. Schafer, E. V. Shuryak and M. Velkovsky, Phys. Rev. Lett. **81**, 53 (1998)
- [20] J. Berges and K. Rajagopal, Nucl. Phys. B **538**, 215 (1999)



- [21] R. D. Pisarski and D. H. Rischke, Phys. Rev. Lett. **83**, 37 (1999)
- [22] G. W. Carter and D. Diakonov, Phys. Rev. D **60**, 016004 (1999)
- [23] R. D. Pisarski and F. Wilczek, Phys. Rev. D **29**, 338 (1984)
- [24] M. A. Halasz, A. D. Jackson, R. E. Shrock, M. A. Stephanov and J. J. M. Verbaarschot, Phys. Rev. D **58**, 096007 (1998)
- [25] S. Ejiri, Phys. Rev. D **73**, 054502 (2006)
- [26] C. R. Allton, M. Doring, S. Ejiri, S.J. Hands, O. Kaczmarek, F. Karsch, E. Laermann and K. Redlich, Phys. Rev. D **71**, 054508 (2005)
- [27] H. Fujii and M. Ohtani, Phys. Rev. D **70**, 014016 (2004)
- [28] J. P. Blaizot, E. Iancu and A. Rebhan, Eur. Phys. J. C **27**, 433 (2003).
- [29] S. A. Gottlieb, W. Liu, D. Toussaint, R. L. Renken and R. L. Sugar, Phys. Rev. Lett. **59**, 2247 (1987); S. Gottlieb et al., Phys. Rev. D **55** 6852 (1997); R. V. Gavai and S. Gupta, Phys. Rev. D **65** 094515 (2002)
- [30] R.V. Gavai and S. Gupta, Phys. Rev. D **73** 014004 (2006); Phys. Rev. D **72** 054006 (2005); Eur. Phys. J. C **43** 31 (2005)
- [31] F. Karsch, S. Ejiri and K. Redlich, Nucl. Phys. A **774**, 619 (2006)
- [32] S. Ejiri, F. Karsch and K. Redlich, Phys. Lett. B **633**, 275 (2006)
- [33] F. Karsch, A. Tawfik and K. Redlich, Phys. Lett. B **571**, 67 (2003); Eur. Phys. J. C **29** 549 (2003)
- [34] Y. Nambu and G. Jona-Lasinio, Phys. Rev. **122**, 345 (1961); Phys. Rev. **124**, 246 (1961)
- [35] U. Vogl and W. Weise, Prog. Part. Nucl. Phys. **27**, 195 (1991)
- [36] S. Klimt, M. Lutz and W. Weise, Phys. Lett. B **249**, 386 (1990)
- [37] T. Hatsuda and T. Kunihiro, Phys. Rept. **247**, 221 (1994)
- [38] M. Buballa, Phys. Rept. **407**, 205 (2005)
- [39] C. Ratti and W. Weise, Phys. Rev. D **70** 054013 (2004)
- [40] C. Ratti, M. A. Thaler and W. Weise, Phys. Rev. D **73**, 014019 (2006)
- [41] L.D. Landau and E.M. Lifshitz, *Statistical Physics*, Course of Theoretical Physics, Vol. 5, (Pergamon Press, New York, 1980) Chapter XIV
- [42] M. Asakawa and K. Yazaki, Nucl. Phys. A **504**, 668 (1989)
- [43] M. Lutz, S. Klimt and W. Weise, Nucl. Phys. A **542**, 521 (1992)
- [44] M. Kitazawa, T. Koide, T. Kunihiro and Y. Nemoto, Prog. Theor. Phys. **108**, 929 (2002)
- [45] F. Karsch, E. Laermann, A. Peikert, Phys. Lett. B **478** 447 (2000); F. Karsch, Nucl. Phys. A **698** 199c (2002)
- [46] C. Sasaki, B. Friman and K. Redlich, arXiv:hep-ph/0611147.
- [47] S. K. Ghosh, T. K. Mukherjee, M. G. Mustafa and R. Ray, Phys. Rev. D **73**, 114007 (2006); C. Ratti, S. Roessner and W. Weise, arXiv:hep-ph/0701091.
- [48] P. Braun-Munzinger, J. Cleymans, H. Oeschler and K. Redlich, Nucl. Phys. A **697**, 902 (2002); J. Cleymans, H. Oeschler, K. Redlich and S. Wheaton, Phys. Rev. C **73**, 034905 (2006)
- [49] D.J. Amit, *Field Theory, the Renormalization Group and Critical Phenomena*, World Scientific, Singapore, 1984
- [50] J.B. Kogut, M.A. Stephanov and C.G. Strouthos, Phys. Rev. D **58**, 096001 (1998)
- [51] B.-J. Schaefer and J. Wambach, hep-ph/0603256
- [52] B. Berndnikov and K. Rajagopal, Phys. Rev. D **61** 105017 (2000)
- [53] Y. Hatta and M.A. Stephanov, Phys. Rev. Lett. **91** 102003 (2003)
- [54] M.D. Elia, A. Di Giacomo and C. Pica, Phys. Rev. D **72** 114510 (2005)
- [55] B. He, H. Li, C. M. Shakin and Q. Sun, Phys. Rev. C **67**, 065203 (2003); B. He, H. Li, C. M. Shakin and Q. Sun, Phys. Rev. D **67**, 114012 (2003)
- [56] A. Erdélyi *et al.*, *Higher transcendental functions*, Bateman Manuscript Project, Vol. 1 (McGraw-Hill, New York, 1953)